Title: Extreme environmental conditions erode coral reef biodiversity and functioning

Authors: Simon J. Brandl[1,2,3,4]*†, Jacob L. Johansen[5,6]†, Jordan M. Casey[3,4], Luke Tornabene[7], Renato A. Morais[8,9], John A. Burt[6]

† indicates shared first authorship

***Corresponding author:** Simon J. Brandl, simonjbrandl@gmail.com,

(ORCID: 0000-0002-6649-2496)

Affiliations:

[1] Department of Biological Sciences, Simon Fraser University, Burnaby, BC, Canada

[2] CESAB - FRB, 5 Rue de l'École de Médecine, 34000, Montpellier, France

[3] PSL Université Paris: CNRS-EPHE-UPVD USR3278 CRIOBE, Université de Perpignan, Perpignan, France

[4] Laboratoire d'Excellence "CORAIL," Perpignan, France

[5] Hawai'i Institute of Marine Biology, University of Hawai'i at Manoa, Kane'ohe, HI, USA

[6] Marine Biology Laboratory, Centre for Genomics and Systems Biology, New York University Abu Dhabi, Abu Dhabi, United Arab Emirates

[7] School of Aquatic and Fishery Sciences and the Burke Museum of Natural History and Culture, University of Washington, Seattle, WA, USA

[8] ARC Centre of Excellence for Coral Reef Studies, James Cook University, Townsville, QLD, Australia

[9] College of Science and Engineering, James Cook University, Townsville, QLD, Australia

Abstract:

Environmentally mediated transformations of ecological communities can influence ecosystem functioning. Coral reef fishes are hypothesized to be vulnerable to environmental extremes, but cascading effects of organismal tolerances on the assembly and functioning of reef fish communities are largely unknown. Here, we compare the world's hottest, most extreme coral reefs in the southern Arabian Gulf to the environmentally benign nearby Gulf of Oman. We show that cryptobenthic reef fishes in the Arabian Gulf are half as diverse and less than 25% as abundant as in the Gulf of Oman, despite comparable benthic composition and live coral cover. Nevertheless, this pattern is not driven by intrinsic organismal temperature tolerances. Rather, impoverished body conditions of populations in the Arabian Gulf and intraspecific differences in the diversity and composition of ingested prey items between locations suggest that reefs in the Arabian Gulf represent an energetically challenging environment that prohibits the persistence of many small-bodied ectotherm species. In turn, this leads to reduced production, transfer, and replenishment of biomass through cryptobenthic fish assemblages. Our results suggest that reefs subject to extreme environmental conditions, as predicted for the end of the 21st century, may face disruptions to their fast-paced bottom-up dynamics, independent of live coral loss.

Introduction:

Why do some species occur in a given location while similar taxa are missing? And how do resulting species assemblages affect rates of ecological processes? As escalating human impacts on the biosphere deplete and re-shuffle biological communities across

ecosystems[1,2], answers to these questions are key to our quest to preserve biodiversity and ecosystem services to humanity[3].

A species' presence at a given location is mediated by a hierarchical interplay between organismal traits (e.g., temperature tolerance, trophic niche), environmental conditions (e.g., temperature, salinity, dissolved oxygen), biotic interactions (e.g. habitat availability), biogeographic history, and stochastic events (e.g., extinction, dispersal)[4–6]. Furthermore, the identity and diversity of species impact rates of ecosystem functioning, including processes that are critical to human well-being, such as primary or consumer productivity[7,8]. However, by modifying abiotic conditions, species' niches, and biotic interactions, global stressors such as climate change can interfere with these dynamics through numerous pathways[9–11]. At the organismal level, changes in environmental factors, such as temperature, affect internal physiological processes in ectotherms (e.g., oxygen consumption)[12], which, if not lethal, will alter organismal energy expenditure[13–15]. Changes in organismal energy demands subsequently drive resource acquisition (e.g. feeding rates, prey species) and how resulting energy is allocated to life-supporting processes (homeostasis), growth, and reproduction[16–18]. Dynamics of energy acquisition and investment, which are often investigated through the lens of ecological niches and fitness, are the basis of modern coexistence theory and critical for our understanding of community assembly dynamics[19] and the rate of ecological processes that underpin energy and nutrient fluxes through ecosystems[20]. Integration across levels of biological organization is, therefore, crucial to understand the effects of global environmental change on our planet's ecosystems[21].

Coral reefs are the most diverse marine ecosystem, and their productivity provides vital services for more than 500 million people worldwide[22]. Scleractinian corals, the foundation species of tropical reefs, show high sensitivity to thermal extremes, which has led to the rapid global decline of coral reef ecosystems[23]. In the wake of losing coral habitat, communities of the most prominent reef consumers, teleost fishes, also decline or shift in composition[24–27], which directly affects the provision of resources to people dependent on reef fisheries[28]. Although recent evidence suggests that some fish species will be able to cope with (or even benefit from) live coral loss, at least in the short-term[28–31], tropical reef fishes are typically adapted to a relatively narrow suite of environmental conditions. Thus, reef fishes may also be vulnerable to the direct effects of climate change on, for instance, sea surface temperatures[13,32,33]. Consequently, the responses of reef fishes to ongoing changes in their environment might be as important as indirect, habitat-mediated responses[34–36].

While other environmental factors (such as salinity or oxygen saturation) have considerable effects on reef fish physiology[37], temperature is by far the most commonly investigated environmental stressor for reef fishes. Despite marked differences in species-specific tolerances to higher temperatures[38–43], most reef fish species suffer from non-lethal[44] adverse physiological, developmental, or behavioral responses when exposed to temperatures outside their normal range. Current understanding suggests long-term deleterious effects on reef fish populations in the wild[34], but few cases of direct temperature-mediated population declines have been documented *in situ* for reef fish communities[45]. One factor that ameliorates the adverse effects of rising temperatures in the wild may be transgenerational acclimation and adaptation, which

92 can enhance the performance of offspring in higher temperatures through
93 developmental, genetic, or epigenetic pathways[36,46]. Transgenerational adaptation has
94 been shown in a few model species[36,46,47], but demands increased energetic
95 investments[46,48]. It is unclear whether this process can truly enhance the survival of reef
96 fishes in competitive, uncontrolled environments and how species-specific temperature
97 tolerance differences may mediate coexistence in ecological communities.
98 Cryptobenthic fishes are the smallest of all reef fishes, rarely exceeding 50mm in
99 maximum body size[49]. They account for almost half of all reef fish species and are
100 numerically abundant and ubiquitous on reefs worldwide[49–52]. Due to their small body
101 size, these fishes have evolved a unique life history strategy of rapid growth, high
102 mortality, and continuous larval replenishment, and play an important role in coral reef
103 trophodynamics[53]. Their small body size and associated life-history also promise
104 exceptional traceability concerning the effects of, and responses to, changing
105 environmental conditions[49]. Limited gill surface area, high mass-specific metabolism,
106 and other physiological challenges resulting from their minute size suggest that
107 cryptobenthics are particularly susceptible to temperature fluctuations[40,49,54]. Due to
108 their limited mobility and close association with the benthos[55], mitigation of temperature
109 extremes through migration is also not viable and otable shifts in cryptobenthic fish
110 community composition have been observed following small-scale changes in the
111 benthic community structure[27,56]. However, the extremely high generational turnover
112 (7.4 generations per year in the most extreme species[53,57]) and prevalence of benthic
113 clutch spawning and parental care[49] may make them ideally suited for transgenerational
114 adaptation to changing conditions[34]. In fact, an extremely fast evolutionary clock has

been implicated as a driver for rapid speciation in cryptobenthic fishes[58], which may permit similarly fast microevolutionary changes (i.e., rapid adaptation). Thus, cryptobenthic fishes may be well-suited to detect the impact of environmental change on organisms and populations, with promising insights into whether transgenerational plasticity or adaptation can provide pathways to the persistence of coral reef fishes in changing oceans.

Here, we quantify cryptobenthic community structure, species- and population-specific physiological and dietary traits, and contributions to ecosystem functioning in the world's hottest, most extreme coral reef environment, the southeastern Arabian Gulf, and we compare the resulting patterns with the spatially proximate, but more thermally moderate, Gulf of Oman. Specifically, the goal of our study was to 1) describe cryptobenthic fish assemblages across the two locations, 2) identify organismal traits that permit or preclude existence in the Arabian Gulf, and 3) determine the consequences of these results for the production, provision, and renewal of cryptobenthic fish biomass[21].

Results:

Between 2010 and 2018, remotely sensed temperature data (MODIS-Aqua, https://oceandata.sci.gsfc.nasa.gov/MODIS-Aqua/) from the studied sites ranged between a minimum of 19.1ºC (Gulf of Oman in 2016) to a maximum of 32.9ºC (Arabian Gulf in 2014) (Fig. S1), with the seven highest temperatures all occurring in the Arabian Gulf. *In situ* data loggers deployed at our study sites[59] recorded summer maximum temperatures of 36ºC (mean daily maximum from 2012 – 2017: 33.7ºC) in the Arabian

Gulf and 34.8ºC (mean daily maximum from 2012 – 2014: 29.9ºC) in the Gulf of Oman, while recording minimum winter temperatures of 17.3ºC (mean daily minimum = 22.0ºC) in the Arabian Gulf and 21.5ºC (mean daily minimum = 23.7ºC) in the Gulf of Oman (Fig. S2). Moreover, in 2012, 2013, and 2014 (for which data were available from both locations), sites in the Arabian Gulf recorded an average of 69.0, 63.7, and 64.3 days per year, respectively, where daily maximum temperatures exceeded 34ºC, while sites in the Gulf of Oman recorded averages of 0.0, 1.0, and 5.0 days, respectively (Table S1)[60]. Thus, maximum temperatures on reefs along the Arabian Gulf coast of the United Arab Emirates closely approach forecasted temperatures for tropical coral reefs at the end of the century[61].While the two locations also differ in several co-varying environmental factors, including salinity, productivity, or reef geomorphology, temperature is commonly considered the strongest environmental force that shapes life in the Arabian Gulf[59–63]. Despite the seemingly unfavorable conditions for tropical reef building corals, corals have persisted in this region for approximately 15,000 years, with the modern coastline harboring coral reef structures for circa 6,000 years[61]. Therefore, the Arabian Gulf represents a useful natural laboratory to examine the capacity of reef organisms to cope with extreme environmental conditions (particularly temperature) and how this influences the diversity and ecological dynamics that underpin modern coral reefs (Fig. 1a,b).

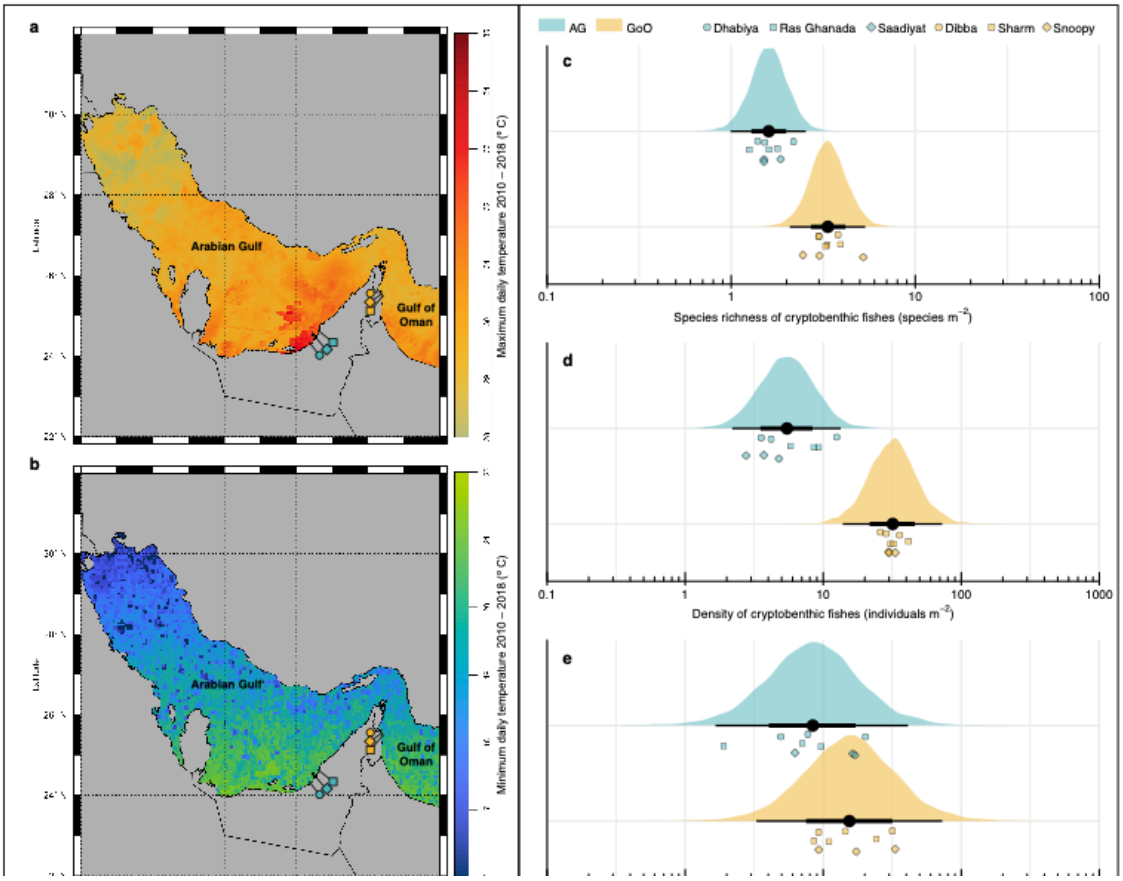

Fig. 1: Map of the study system and community structure of cryptobenthic reef fish communities in the Arabian Gulf (AG) and Gulf of Oman (GoO). (**a–b**) Maximum and minimum daily temperature estimates for the AG and GoO between 2010 and 2018 (obtained from MODIS Aqua; https://oceandata.sci.gsfc.nasa.gov/MODIS-Aqua/Mapped/Daily/4km/sst), with the study sites indicated. (**c**) Species richness and (**d**) abundance of cryptobenthic reef fishes was markedly lower on reefs in the AG, while (**e**) biomass did not substantially differ between the two locations. Density curves represent predicted values based on 1,000 draws from Bayesian hierarchical linear models testing for differences between locations, while black caterpillar plots represent their means, 50%, and 95% credible intervals. Circles, squares, and diamonds represent raw values from the respective sites in each location, jittered on the y-axis.

Cryptobenthic reef fish assemblages markedly differed between the Arabian Gulf and the Gulf of Oman. Reefs in the Arabian Gulf harbored less than half the richness (7.11 ± 0.5 SE species m^{-1} vs. 15.9 ± 1.8 SE species m^{-1}; Bayesian hierarchical model estimate: *Gulf of Oman:* $\beta = 0.73$ [0.44, 1.01; lower and upper 95% credible interval]) and less than a quarter the abundance (28.3 ± 6.6 SE individuals m^{-1} vs. 149.0 ± 13.5 SE individuals m^{-1}; *Gulf of Oman:* $\beta = 1.77$ [1.03, 2.58]) of cryptobenthic fishes (Fig.

1c,d), but standing biomass estimates were comparable (*Gulf of Oman:* β = 0.63 [-0.54, 1.71]; Fig. 1e). Similarly, the composition of cryptobenthic communities greatly varied between the two locations (Fig. 2a), with no overlap among convex hull polygons in the non-metric multidimensional scaling (nMDS) ordination and a strong effect of *Location* in the PERMANOVA using a site-by-species dissimilarity matrix (*Location*: *df* = 1, *F* = 13.58, *P* = 0.001, *R2* = 0.46). There were 13 unique species in the Arabian Gulf, 29 unique species in the Gulf of Oman, and 16 species shared among the two locations. Importantly, of the 29 unique Gulf of Oman species, 89.7% have been recorded from the northern Arabian Gulf in Kuwait and Saudi Arabia (but not the southeastern region), where summer conditions are much less extreme[64] (Fig 1; Table S2). In contrast to the cryptobenthic fish community, there were no statistical differences in coral cover (Bayesian hierarchical model: *Gulf of Oman:* β = 0.02 [-1.30, 1.42]) nor overall benthic community structure as revealed by a PERMANOVA (*Location*: *df* = 1, *F* = 1.63, *P* = 0.187, *R2* = 0.09; Fig. 2b). Thus, despite broadly comparable benthic community composition and live coral cover (two commonly quantified metrics), cryptobenthic fish assemblages strongly differed between the two locations. Notably, reefs in the two locations may also differ in their geomorphology, structural complexity, or fine-scale benthic composition, which was not considered in the present study but may have some effect of cryptobenthic fish assemblages.

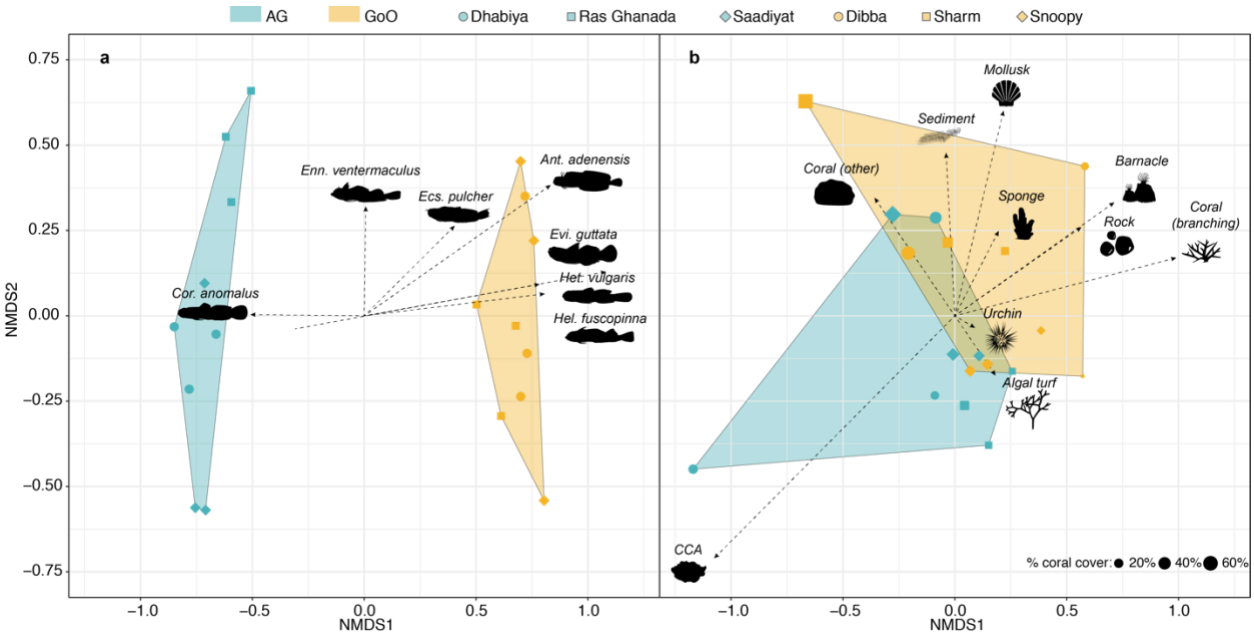

Fig. 2: Community composition of cryptobenthic reef fishes and benthic functional/taxonomic groups in the Arabian Gulf (AG) and Gulf of Oman (GoO). (**a**) Biplot of a non-metric multidimensional scaling (nMDS) ordination on cryptobenthic fish communities, with the arrows indicating the position and strength of the seven most important species. (**b**) Biplot of an nMDS on benthic functional groups, with the influence of all groups indicated with arrows. Convex hull polygons delineate the two locations. Each point represents a sample station at a particular site, with the shape size in (**b**) scaled by percent live coral cover. CCA = crustose coralline algae.

We then tested whether organismal temperature tolerance can explain the absence of three Gulf of Oman species (*Helcogramma fuscopinna*, *Eviota guttata*, and *Hetereleotris vulgaris*) from the thermally extreme southeastern Arabian Gulf, despite their recorded presence in more benign parts of the Arabian Gulf. We also examined the potential for intraspecific plasticity in two species with populations in both locations (*Enneapterygius ventermaculus* and *Ecsenius pulcher*). Species-specific critical thermal tolerance limits did not explain the absence of three common Gulf of Oman species in the Arabian Gulf (Fig. 3). The mean critical thermal maximum tolerance limits (ct_{max}) of all six tested species, regardless of origin, equaled or surpassed the maximum summer temperatures typically recorded in the Arabian Gulf (36.0ºC). *Helcogramma fuscopinna*

(a Gulf of Oman species) had the lowest heat tolerance at 36.0 ± 0.11ºC, while *Coryogalops anomolus* from the Arabian Gulf had the greatest heat tolerance (38.4 ± 0.06ºC). While there were no population differences in heat tolerance for *E. ventermaculus* (possibly due to limited samples from the Gulf of Oman), the Arabian Gulf population of *E. pulcher* showed slightly greater heat tolerance (0.6ºC) than their Gulf of Oman counterparts (37.9ºC ± 0.05ºC SE vs. 37.3ºC ± 0.06ºC SE), providing some evidence for enhanced thermal tolerance in this species. Despite considerable interspecific differences and some evidence for intraspecific thermal plasticity (Table S3), mean predicted maximum posterior heat tolerances of all species restricted to the Gulf of Oman were within the 95% bounds of the species present in the Arabian Gulf.

In terms of critical thermal minima (ct_{min}), all species, regardless of origin, tolerated the minimum winter temperature of the UAE Arabian Gulf at 17.3ºC. Among individuals sampled from the Gulf of Oman population, *E. pulcher* had the greatest tolerance to cold (ct_{min} = 11.3 ± 0.1ºC), while *E. ventermaculus* had the poorest tolerance (13.3 ± 0.1ºC). The cold-tolerance of *E. ventermaculus* in the Arabian Gulf (12.3º C ± 0.06º C SE) exceeded its Gulf of Oman counterpart (13.3ºC ± 0.10 SE) (Table S4), which provides evidence from a second population for intraspecific plasticity in thermal tolerances across the two locations. Although there were again species-specific differences in the critical thermal minimum, mean cold tolerances of all Gulf of Oman species also fell within the 95% credible bounds of the species present in the Arabian Gulf (Fig. 3a).

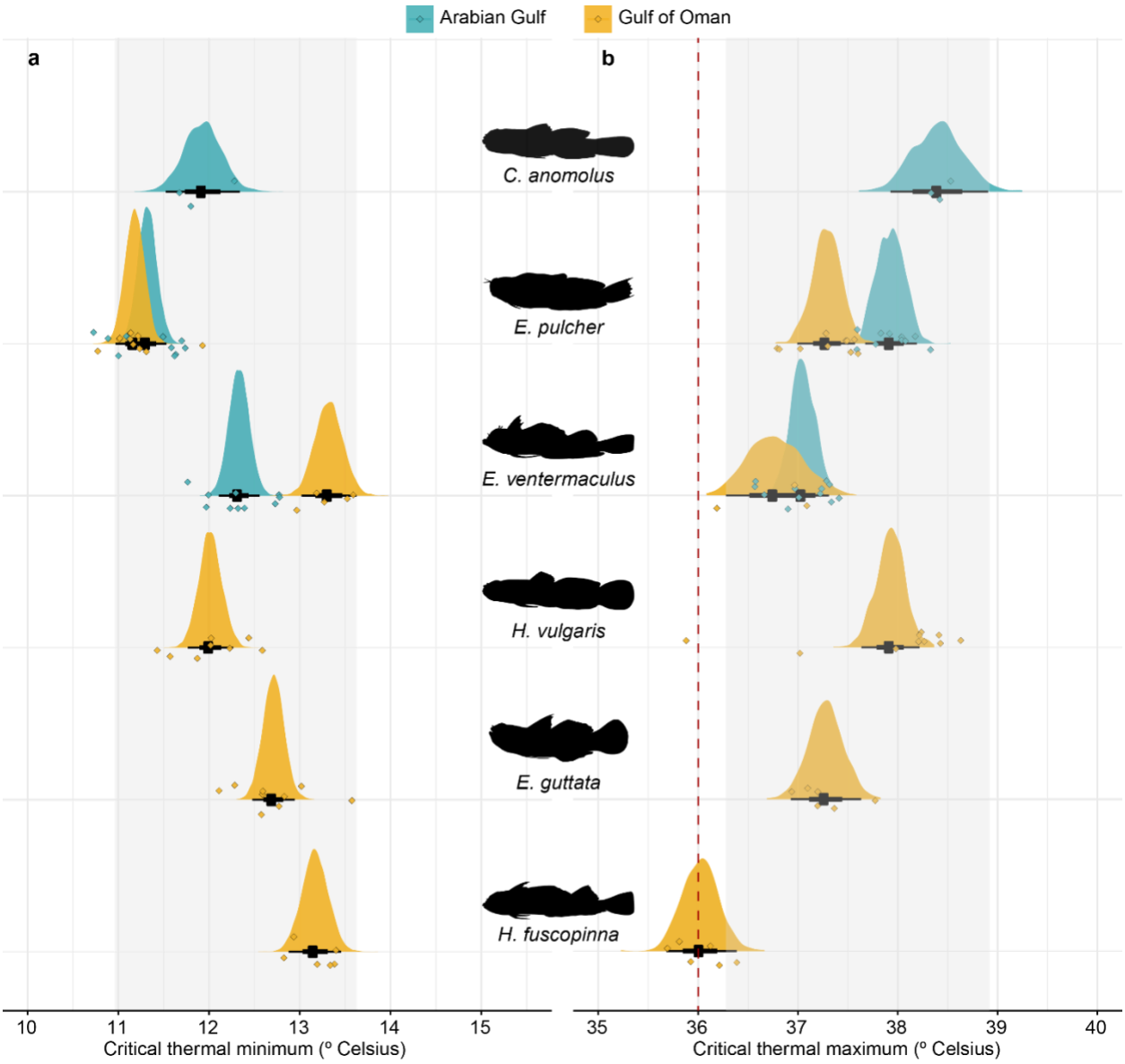

Fig. 3: Critical thermal tolerance limits of cryptobenthic fish species from the Arabian Gulf and Gulf of Oman. (**a**) Average critical thermal minima ranged between 11.9 ºC and 13.3 ºC, well below the minimum recorded winter temperature for the southern Arabian Gulf (16.0 ºC). (**b**) Average critical thermal maxima ranged between 36.0 ºC and 38.4 ºC, but they were above or equal to the maximum recorded summer temperature in the Arabian Gulf (36.0 ºC; red dashed line). Density curves represent fitted values based on 10,000 draws from Bayesian linear models that test for differences among all populations, while black caterpillar plots represent their means, 50%, and 95% credible intervals. Diamonds represent raw values, jittered on the y-axis. Grey boxes delineate the range of the 95% credible intervals obtained for the three species present in the Arabian Gulf.

To further examine potential drivers of cryptobenthic community structure, we quantified prey ingestion in the two locations using gut content DNA metabarcoding

252 across 88 individuals belonging to six species (*C. anomolus*, *E. pulcher*, and *E.*
253 *ventermaculus* [Arabian Gulf and Gulf of Oman populations]; *Antennablennius*
254 *adenensis*, *Eviota guttata*, and *Hetereleotris vulgaris* [Gulf of Oman only]). We targeted
255 the cytochrome *c* oxidase subunit I (COI) gene region with primers that preferentially
256 amplify metazoans and the 23S rRNA gene region with primers designed to amplify
257 algae. Across all examined fishes, COI metabarcoding yielded a total of 547 unique
258 operational taxonomic units (OTUs), while 23S metabarcoding yielded 3,009 unique
259 exact sequence variants (ESVs). Bipartite dietary network trees and modularity
260 analyses for the COI marker showed strong separations between the Arabian Gulf and
261 Gulf of Oman populations (Fig. 4). The COI network contained five distinct modules
262 (modularity = 0.472), with 92.3% of individuals from the Arabian Gulf distributed across
263 two modules. Module V contained seven out of ten individuals of *C. anomolus* from the
264 Arabian Gulf, 8 out of 9 individuals of *E. ventermaculus* from the Arabian Gulf, and one
265 *E. guttata* from the Gulf of Oman. The remaining individuals of *C. anomolus* and *E.*
266 *ventermaculus* from the Arabian Gulf clustered with *E. pulcher* from the Arabian Gulf
267 (five out of seven), four Gulf of Oman individuals of *C. anomolus*, and a single *H.*
268 *vulgaris* in module II (Fig. 4a,b). The 23S marker also revealed five modules (modularity
269 = 0.359) but showed an even stronger regional separation. All individuals from the
270 Arabian Gulf (except for one individual of *C. anomolus*) were united in a single module
271 (module III), which contained no Gulf of Oman individuals (Fig. 4c,d). While some
272 species separated into distinct modules, location specific differences superseded
273 taxonomic boundaries. With the exception of *C. anomolus*, species occurring in both

locations showed strong dietary differences, while broadly overlapping with other species in the Gulf of Oman.

Prey diversity rarefaction curves in the Gulf of Oman showed that *E. pulcher*, a purportedly herbivorous species[66], ingested the widest variety of animal prey species (COI marker), followed by *E. ventermaculus* (Fig. S3). For both species, Gulf of Oman populations consumed a higher diversity of prey items than Arabian Gulf populations. Only *C. anomolus* showed no clear difference in extrapolated values (although diversity was higher for Gulf of Oman populations for the interpolated value). For algal prey items (23S marker), prey diversity was again higher in Gulf of Oman populations of *E. pulcher* and *E. ventermaculus*, while the opposite was evident for *C. anomolus*. Overall, Gulf of Oman populations of *E. ventermaculus* ingested the highest autotroph prey diversity, followed by Arabian Gulf populations of *C. anomolus*.

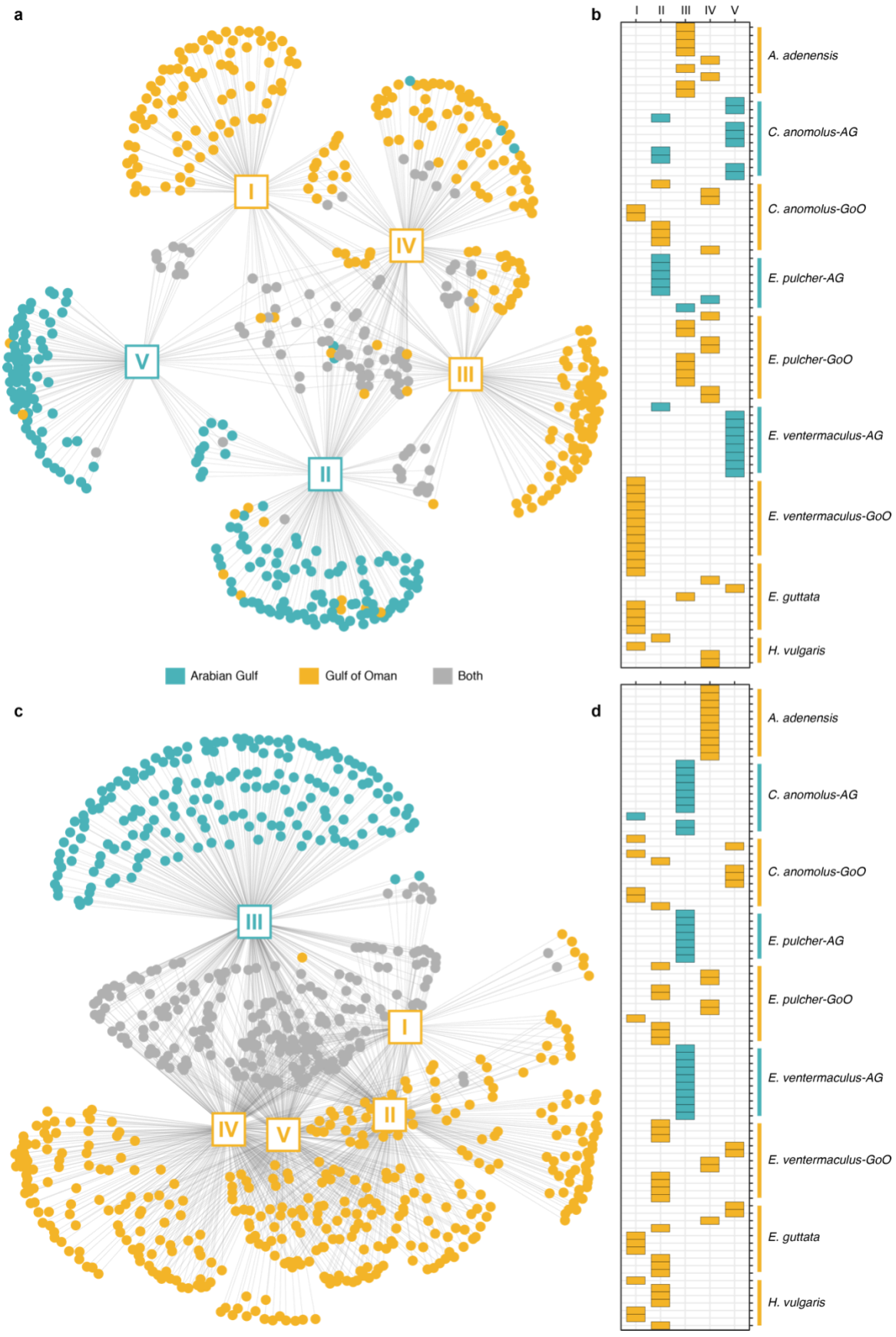
a
b
c
d
I
II
III
IV
V
A. adenensis
C. anomolus-AG
C. anomolus-GoO
E. pulcher-AG
E. pulcher-GoO
E. ventermaculus-AG
E. ventermaculus-GoO
E. guttata
H. vulgaris
Arabian Gulf
Gulf of Oman
Both

287

Figure 4: Diet network trees and modularity mosaics showing differences in ingested prey items and individual-based module membership for COI (a,b) and 23S (c,d) markers. (a,c) Squares with roman numerals represent the recovered modules as nodes in the network tree, while dots represent unique prey items. Blue dots are OTUs (COI) or ESVs (23S) found only in individuals from the Arabian Gulf, gold symbols are from the Gulf of Oman individuals, and grey symbols represent prey items found in individuals from both locations. **(b,d)** Results of the modularity analysis with modules (I-V) as columns and individuals within each species as rows. Colored tiles indicate membership in a given module.

We further examined the potential organismal and ecosystem-wide energetic consequences of thermal regimes and resource availability between the two locations by first assessing length-weight relationships of three co-occurring species, and then by modeling individual-based growth and mortality to estimate community-wide biomass cycling. We employed Bayesian linear models to test the effects of total length (*TL*) and *Location* on *Weight*, which showed clear effects of *Location* across all species, with Gulf of Oman populations consistently having higher weights for a given body length (*E. ventermaculus*: *Gulf of Oman:* β = 0.16 [0.13, 0.19], *E. pulcher*: *Gulf of Oman:* β = 0.19 [0.14, 0.25]), and *C. anomolus*: *Gulf of Oman:* β = 0.15 [0.09, 0.21] (Fig. 5). Specifically, at each species' mean total length, our model predictions show that individuals of *E. ventermaculus*, *E. pulcher*, and *C. anomolus* were 67.2%, 62.2%, and 10.0% heavier in the Gulf of Oman, respectively. Notably, empirical values for the largest individuals of *C. anomolus* from the Arabian Gulf were consistently below the model fit, suggesting worse body conditions than predicted by the model and substantially worse body conditions than Gulf of Oman individuals of comparable size (Fig 5b). In contrast, no clear differences emerged between the abundances of the three species' populations across locations (effect size uncertainties intersected zero), although *E. ventermaculus* (*Gulf of Oman:* β = 0.89 [-1.08, 2.86) and *E. pulcher* (*Gulf of Oman:* β = 3.46 [-0.42,

9.93]) showed a trend toward lower abundances in the Arabian Gulf, while *C. anomolus* exhibited the opposite trend (*Gulf of Oman:* β = -0.94 [-3.82, 1.69]).

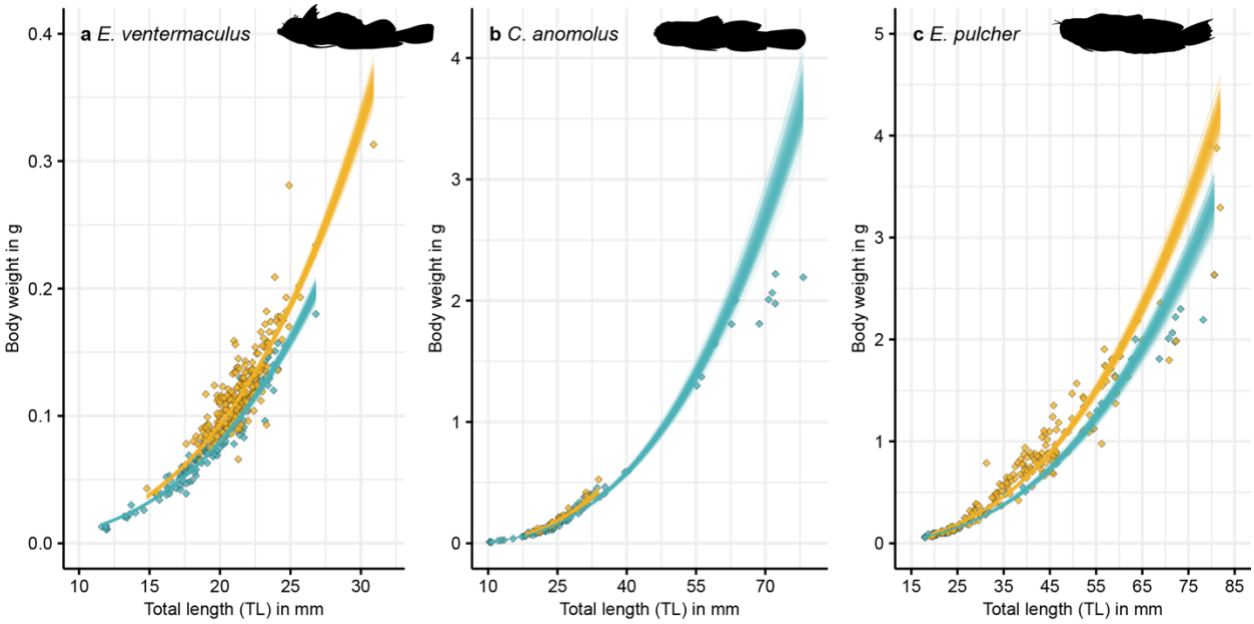

Figure 5: Relationships between total length (TL) and body weight in populations of *Enneapterygius ventermaculus* (a), *Coryogalops anomolus* (b), and *Ecsenius pulcher* (c) in the Arabian Gulf (blue) and Gulf of Oman (gold). Each line represents a fitted draw from 500 iterations based on the posterior parameters from a Bayesian model regressing length against weight (thus showing model fit uncertainty). Diamonds represent raw values for individual fishes.

Finally, modeling individual-based growth and mortality for cryptobenthic fish communities at each site revealed strong differences between the Arabian Gulf and Gulf of Oman in the ecological dynamics that underpin reef ecosystem functioning (Fig. 6). Biomass production was almost one order of magnitude lower on reefs in the Arabian Gulf (0.038 ± 0.014 g d^{-1} m^{-2}) compared to the Gulf of Oman (0.231 ± 0.025 [mean ± SE] g d^{-1} m^{-2}), while consumed biomass was more than five times lower (0.007 ± 0.001 g d^{-1} m^{-2} vs. 0.039 ± 0.015). Turnover was also lower in the Arabian Gulf (0.006 ± 0.005 % d^{-1}) compared to the Gulf of Oman (0.017 ± 0.005 % d^{-1}). Therefore, reefs in the two locations exhibit contrasting productivity dynamics at various levels of organization. In

the Arabian Gulf, individual fishes accumulate less body mass per millimeter of body length and collectively, cryptobenthic communities produce, provide, and replenish consumer biomass at much lower rates than Gulf of Oman communities.

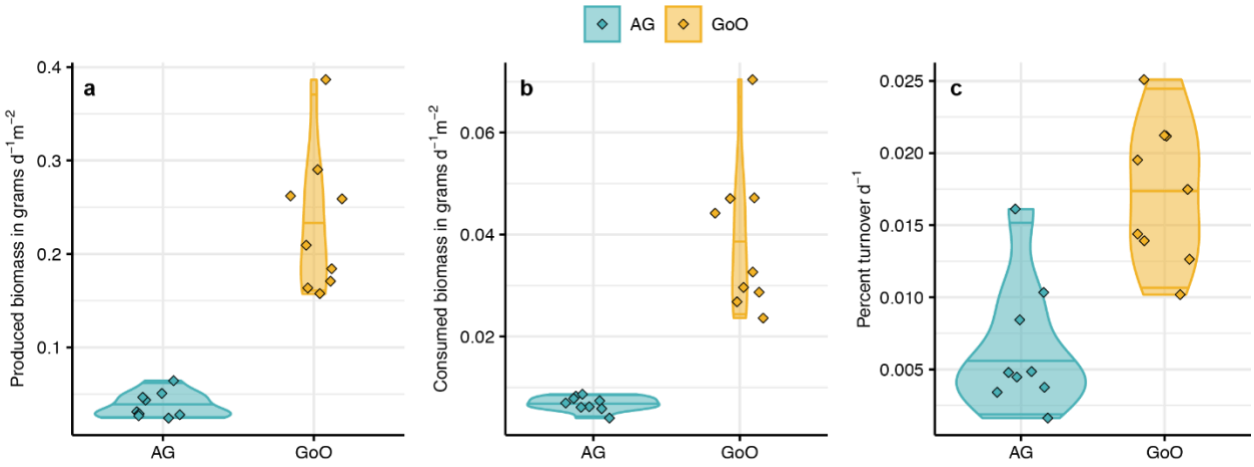

Figure 6: Model estimated biomass production, consumption, and turnover in cryptobenthic fish assemblages across the two locations. (**a**) Produced biomass (grams of fish tissue grown per day and m_2). (**b**) Consumed biomass (grams of fish tissue perished per day and m_2). (**c**) Percent turnover (renewal of produced and consumed biomass per day). Violin plots and lines represent medians and variance estimates (95% quartiles) for the three metrics across the two locations. Diamonds represent values for each sampled cryptobenthic reef fish community across the six sites (three per site).

Discussion:

As rapid environmental change sweeps across the Earth's ecosystems, understanding the processes that underpin local community structure and ecosystem functioning is urgent. Here, we show that cryptobenthic fishes on the world's most environmentally extreme reefs in the southeastern Arabian Gulf have reduced diversity, abundance, and body condition compared to reefs with more moderate temperatures in the nearby Gulf of Oman, despite similarities in live coral cover and benthic community structure. While we found some evidence for intraspecific thermal plasticity, which may enable survival

in Arabian Gulf conditions, species-specific temperature tolerances may not be the main driver of species presence/absence in the Arabian Gulf. Rather, poor body condition in Arabian Gulf populations alongside intraspecific differences in the diversity and composition of ingested prey items across the two locations indicate that the biotic and abiotic conditions in the Arabian Gulf foster an energetically challenging environment that prevents the persistence of many small-bodied ectotherms. This has cascading consequences for ecosystem-scale energy and nutrient fluxes, as even conservative estimates of cryptobenthic reef fish productivity in the Arabian Gulf are an order of magnitude lower than the Gulf of Oman. Our results indicate that cryptobenthic reef fish assemblages on future coral reefs may be shaped by species-specific individual energy deficits that decrease the rate of biomass production, transfer, and renewal through small vertebrate consumers, thereby eroding a cardinal component of heterotrophic coral reef productivity[53].

Organismal responses

As the smallest and shortest-lived marine vertebrates, responses of cryptobenthic fishes to extreme temperatures should be easy to trace[49]. Yet, critical thermal tolerances of all tested species from both locations were equal to or greater than the extreme maximum summer temperatures of the southeastern Arabian Gulf[41,44,67]. The high intrinsic temperature tolerance of species from the thermally moderate Gulf of Oman aligns with previous results of high, short-term critical thermal tolerances in cryptobenthics[41]. Furthermore, provided that self-recruitment is high for cryptobenthic fishes[53], swift generational turnover in cryptobenthic fishes could facilitate transgenerational thermal

plasticity and increased thermal tolerance[53,57]. Collectively, this should have permitted their colonization and persistence in the geologically young southeastern Arabian Gulf[62] since no hard biogeographic boundary exists between the Gulf of Oman in the Arabian Gulf[63]. Indeed, 26 out of 29 (89.7%) cryptobenthic fish species from the Gulf of Oman that were absent from the southeastern Arabian Gulf (where temperatures are highest in the summer, but moderate in the winter) have been recorded in the cooler Arabian Gulf regions of Saudi Arabia and Kuwait (Table S2)[64,68,69]. Thus, neither thermal tolerances to short-term temperature extremes nor biogeographic history are likely to drive the observed depauperate cryptobenthic communities on Earth's hottest coral reefs. While it is possible that organismal tolerances to other environmental factors, such as elevated salinity, may play a part in the observed patterns, temperature is generally considered to be the primary environmental force that shapes Arabian Gulf communities[60,61,70].

In the absence of a direct lethal effect of temperature or other environmental factors, our results suggest that more nuanced forces act upon individual energy budgets via transgenerational acclimation or adaptation and available prey resources. Transgenerational acclimation or adaptation of fishes to environmental extremes can come with substantial energetic costs[36,46,71] that are frequently reflected in reduced body condition, even when subsequently exposed to more moderate environmental regimes[72–74]. These costs (necessitated by either extreme temperatures or overall environmental variability) are evident in the lower mass per unit body length of Arabian Gulf populations in the three examined species. At the time of sampling (end of spring), two out of three species were more than 60% lighter at their mean body length in the

Arabian Gulf, suggesting substantial deficits in condition. Since temperatures are generally comparable between the two locations in the spring (Fig. S2), and spring is typically when animals accrue body mass between seasonal extremes, the poor body condition found in Arabian Gulf populations may be a consequence of transgenerational processes that enable survival, but hamper physical condition (e.g., up-regulation of metabolic rates, liver inflammation[46]).

This energetic challenge may be exacerbated by fundamentally different prey resources and reduced prey diversity; indeed, gut content metabarcoding revealed a different and narrower range of prey resources ingested by individuals from the Arabian Gulf. Shifts in prey composition often necessitate changes in digestive efficiency that may require radical physiological or morphological adjustments, ultimately affecting species' energy budgets[75,76]. Furthermore, a lower diversity of prey items can reduce individual and population persistence[77,78]. Naturally, energetic challenges will be even greater if prey in the Arabian Gulf have less favorable nutritional profiles or energy densities[79]. While we did not investigate differences in diet quality (i.e., nutrient content, energetic yield) or quantities of prey across locations, large reef fish species in the Arabian Gulf have been shown to ingest unusual diets dominated by nutritiously poor benthic invertebrates[80]. Collectively, our findings suggest that transgenerational acclimation to environmental extremes and their associated energetic costs may not be a viable strategy if environments are resource-limited, either in quality, quantity or both. Thus, although transgenerational adaptation to environmental change has been shown to enable survival in controlled laboratory conditions[36,46], its role appears limited in the

wild, where animals continuously engage in costly activities such as foraging or escaping predators[72].

The role of deeply rooted evolutionary processes in permitting persistence in extreme environments, rather than short-term plasticity, is supported by the goby *Coryogalops anomolus*. *C. anomolus* was the only species to show weakly distinct prey composition between locations and higher autotroph prey richness in the Arabian Gulf, and had a higher abundance and larger body size in the Arabian Gulf as compared to the Gulf of Oman. Furthermore, compared to *E. pulcher* and *E. ventermaculus*, differences in body condition between locations were weak for *C. anomolus*. As opposed to most dominant cryptobenthic genera in the Arabian Gulf and Gulf of Oman (e.g. *Ecsenius, Eviota, Enneapterygius*, etc.), the goby genus *Coryogalops* belongs to a clade that contains many non-reef associated species from comparatively extreme habitats[81,82] For example, *Coryogalops* often inhabit tidepools and other shallow environments exposed to fluctuating temperatures and salinity where they rely on a sedentary lifestyle with low energetic costs[83,84]. Thus, the persistence of thriving *C. anomolus* populations in the southeastern Arabian Gulf may reflect deeper evolutionary rooting in extreme environments.

Our results indicate that species-specific capacities to cope with the energetic costs of inhabiting extreme environments, rather than the direct effects of temperature *per se* or its effect on benthic community structure (cf.[67]), underpin the limited diversity and abundance of cryptobenthic fishes on these extreme reefs. For cryptobenthics, which already exhibit high energetic demands per gram of body mass for homeostasis and rapid growth[49], augmented energetic costs appear to represent a significant

challenge. Along with environmentally-driven differences in prey composition and diversity (and possible reductions in nutritional value or energetic densities), this 'energetic double jeopardy' may represent an insurmountable obstacle for many cryptobenthic species. Further decreases in body size (a universal physiological response to warmer temperatures[15,73]) might simply not be possible for many cryptobenthic reef fishes that are already at or near the physical minimum body size for vertebrates[49,54,85]. Therefore, our findings from small-bodied tropical ectotherms in a natural setting suggest that more extreme environmental conditions, as predicted due to climate change, may have severe consequences on organismal performance[86,87], with cascading effects on species persistence and community assembly[88].

Ecosystem-scale consequences

The organismal responses that govern community assembly in the southeastern Arabian Gulf create a sobering perspective on coral reef ecosystem functioning in a more extreme, rapidly warming ocean. Coral reefs are highly productive marine ecosystems[89] that are sustained through a variety of energetic pathways[90–93]. Among these pathways, benthic productivity[94] and its assimilation and transfer through cryptobenthic reef fishes represents an important bottom-up flux of energy and nutrients to higher trophic levels[53]. The differences in biomass production, transfer, and turnover between cryptobenthic fish communities in the Arabian Gulf and Gulf of Oman suggest that the role of cryptobenthics as vectors of energy and nutrients to larger consumers may be stymied in extreme environments. In fact, yearly productivity estimates for cryptobenthic fishes in the Arabian Gulf may be even lower than our model suggests

due to the decreased individual-level production of body mass per unit body size and the influence of seasonality effects on growth[95]. Yet, neither environmental limits on the growing season, nor decreased individual mass per unit body size were considered in the model. Inclusion of these factors would likely further reduce productivity estimates for the Arabian Gulf reefs.

The Gulf of Oman reefs included in this study may be particularly productive environments due to seasonal upwelling[96], and indeed, our estimates of cryptobenthic productivity exceeded estimates for a degraded but species-rich reef on the Australian Great Barrier Reef (GBR) (2.31 vs. 0.64 kg $ha^{-1}d^{-1}$)[97]. In contrast, even the optimistic estimate of 0.38 g $ha^{-1}d^{-1}$ for the Arabian Gulf compared poorly with the same degraded GBR-reef. Notably, the study site on the GBR had undergone a sequence of severe disturbances[97], yet it retained a diverse assemblage of cryptobenthic fish species that were likely able to satisfy their energetic demands due to benign temperature profiles[26]. At the time of our survey, reefs in the Arabian Gulf had undergone extensive bleaching in previous years[98–101], which may have negatively affected the diversity and abundance of cryptobenthic fishes compared to the less disturbed reefs in the Gulf of Oman[24,102,103]. Furthermore, larger-scale structural differences between reef outcrops in the Gulf of Oman and the Arabian Gulf may affect our community-wide estimates. However, the lack of difference in benthic community structure observed between regions suggests that benthic structure was at least not a primary driver of the observed patterns. Although the loss of some specialist cryptobenthic species has been reported after substantial live coral cover loss[98,104], previous studies have not detected substantial

short-term changes in either small reef fish richness and abundance or in overarching ecosystem productivity[27,29,31,56,98].

Our results showcase an imminent threat to cryptobenthic reef fishes and their role for coral reef functioning: many of the world's smallest marine ectotherms may struggle to compensate for increasing costs of growth and homeostasis as they adapt to more extreme environmental regimes. As a consequence, small consumer productivity, energy transfer, and replenishment of biomass at the bottom of the fish food chain may decrease under climate change[15]. Analogous to cryptobenthics, the Arabian Gulf harbors less diverse and abundant communities of large reef fishes compared to nearby locations with more moderate temperatures[70,105]. It remains unresolved whether these patterns are driven by similar mechanisms as proposed herein (e.g., an energetic filtering effect on large fish species) or relate to decreased productivity at lower trophic levels. Yet, in light of the hypothesized importance of small vertebrate consumers in global food webs[106] and the unique ecological role of cryptobenthics in coral reef trophic dynamics[53], the effects of elevated temperature on cryptobenthic fish assemblages may considerably reduce ecosystem functioning on future coral reefs.

Methods:

Field sampling

We studied cryptobenthic fish communities in two locations that dramatically differ in their annual temperature profiles. Temperatures in the Arabian Gulf (Dhabiya: 24.36383º, 54.10121º; Ras Ghanada: 24.84743º, 54.69235º; Saadiyat: 24.65771º, 54.48691º) are extremely hot, with summer maximum temperatures reaching up to or

above 36 ºC, while winter minimum temperatures fall to 16 ºC. In contrast, temperatures in the Gulf of Oman (Dibba Rock: 25.55378º, 56.35694º; Sharm Rock: 25.48229º, 56.36695º; Snoopy Rock: 25.49210º, 56.36401º) lie within more typical coral reef temperature profiles throughout the year, ranging from 32 ºC to 22 ºC [63]. Notably, the sampled reefs in the Arabian Gulf are at the extreme end of high maximum summer temperatures, while being relatively benign concerning the low winter temperatures in the rest Arabian Gulf (Fig. 1a,b). At the time of sampling, temperatures between the two locations were between 27ºC and 29ºC at both locations. All *in situ* temperature data (Fig. S2) were obtained from HOBO data loggers deployed at the respective sites (cf.[59]).

In April and May of 2018, we sampled six reefs (hereafter *site*) in the southeastern Arabian Gulf and northwestern Gulf of Oman (three sites per location). At each site, we sampled three distinct reef outcrops for cryptobenthic reef fishes using enclosed clove oil stations[50,107], covering an average of 4.63 ± 0.38 and 4.73 ± 0.16 m^2 in the Arabian Gulf and Gulf of Oman, respectively, for a total of 18 community samples. Since our sampling was not replicated temporally, we cannot exclude the possibility of annual changes in cryptobenthic communities in the Arabian Gulf. Nevertheless, the lack of records for many of the species found in the Gulf of Oman in the southeastern Arabian Gulf indicates that the depauperate nature of cryptobenthic assemblages in this region is not a function of our sampling at a single point in time. For each station, we covered a reef outcrop with a fine-mesh, bell-shaped net (2.74 m in diameter), weighted by a chain on the bottom. We then covered the same area with an impermeable bell-shaped tarpaulin, also weighted by a chain on the bottom. Then, three to four divers inoculated the area under the net with two liters of clove-oil:ethanol solution (1:5) using

collapsible spray bottles (clove bud oil: Jedwards International, Inc., Braintree, MA, USA). Upon emptying the entire solution and a short wait period to allow the clove oil to disperse and take effect (approximately 2-3 mins), we removed the tarpaulin and gently peeled back the net while collecting all fishes found within the inoculated area with tweezers. We searched the entire area, including inside caves and crevices until five minutes passed without a single diver collecting any additional fishes. We placed all fishes into Ziplock bags, brought them to the surface, euthanized them with a clove-oil overdose, and immediately placed them into an ice-water slurry until processing and preservation. At the end of each day, all specimens were brought to the laboratory at NYUAD or the Radisson Blu hotel in Fujairah. To quantify benthic community structure, we used a haphazardly placed 20×20cm PVC-quadrat to frame and take five photographs of the benthos at each sampled outcrop.

In addition to the quantitative samples obtained from the clove-oil stations, we collected cryptobenthic fish individuals for thermal tolerance trials using roving diver collections. Specifically, two divers, each equipped with spray bottles of clove-oil:ethanol solution, a dipnet, and Ziplock bags, searched the reef for cryptobenthic fishes across three species in the Arabian Gulf (*Coryogalops anomolus*, *Ecsenius pulcher*, and *Enneapterygius ventermaculus*) and six species in the Gulf of Oman (*C. anomolus*, *E. pulcher*, and *E. ventermaculus* plus *Eviota guttata*, *Helcogramma fuscopinna*, and *Hetereleotris vulgaris*). Upon locating an individual or identifying a suitable microhabitat in which a fish was suspected, the diver applied the clove-oil solution until the fish showed signs of anesthesia. At the earliest opportunity, we caught the fish with a dipnet and placed it into a ziplock bag. Upon completion of the dive, all

559 fishes were placed in small holding tanks equipped with air stones and periodically
560 replenished with fresh seawater. Upon completion of all collections, fishes were brought
561 to the seawater laboratory facilities at NYUAD. All roving diver collections were
562 performed at Dhabiya Reef (Arabian Gulf) and Snoopy Rock (Gulf of Oman).
563
564 *Laboratory processing*
565 For samples obtained from the enclosed clove-oil stations, we followed an established
566 protocol that involved photographing, identifying, recording, measuring, weighing and
567 preserving each specimen[50]. To photograph the fishes, we placed each individual in a
568 small photo tank and used a Nikon D300 DSLR camera with an AF-S Micro Nikkor
569 60mm macro lens (f/2.8G ED; Nikon Inc., Melville, NY, USA) against a black or white
570 background. We measured each individual to the nearest 0.1mm using digital calipers
571 and weighed the individual (wet weight) to the nearest 0.001 grams on a precision
572 jewelry scale. We preserved all individuals in 95% ethanol, either separately or in lots
573 with conspecifics. A subset of the samples was shipped to the University of Washington
574 Fish Collection, where they were cataloged, while the rest were retained and archived at
575 NYUAD.
576
577 *Benthic photo analysis*
578 For the benthic photographs, we created a grid with 16 equally spaced points which we
579 superimposed on every photograph. We then categorized the benthos at each of the
580 points into functional groups, including barnacles, bleached corals, crustose coralline
581 algae, dead coral, hydroids, branching, encrusting, foliose, and massive live coral,

582 mollusks, bare rock, soft sediment, sponges, algal turf, and sea urchins. Whenever
583 visual identification was not possible (due to obstruction, shading, or blurriness), we
584 categorized the point as “unidentifiable” (n = 69 out of 1,440). All photographs with the
585 grid superimposed are accessible with the raw data of the paper.
586
587 *Critical thermal maximum and minimum trials*
588 We examined individual temperature tolerances by using critical thermal maximum
589 (CT_{max}) and minimum (CT_{min}) trials[108]. We transported all fishes caught during roving
590 diver collections to the wet laboratory facilities at NYUAD and housed them for at least
591 48 hours in large holding tanks. Trials took place from the 9th to 13th of May of 2018. For
592 the trials, a haphazardly selected subset of individuals was moved from the holding
593 tanks into separate chambers filled with seawater at ambient temperature and salinity.
594 Then, after providing individuals with a 15-minute settlement period, we incrementally
595 decreased (CT_{min}) or increased (CT_{max}) the water temperature within the chambers
596 while keeping all other parameters constant. Specifically, we lowered or increased the
597 temperature by 0.1º C every minute[108] while keeping all fishes under constant
598 observation. Critical endpoints were classified as loss of equilibrium or uncontrolled
599 swimming without a righting response for two seconds or more[108]. When individuals
600 reached their critical endpoints, they were immediately removed, euthanized with a
601 clove-oil overdose, measured, weighed, and photographed. In total, we processed 60
602 individuals across six species for CT_{max} trials, and 62 individuals across the same
603 species for CT_{min} trials. Specific sample sizes are provided in the supplementary
604 material (Table S5).

Gut content DNA metabarcoding

We processed a subset of individuals across six species (*A. adenensis*, *C. anomolus*, *E. pulcher*, *E. guttata*, *E. ventermaculus*, and *H. vulgaris*) for gut content DNA metabarcoding at the University of Washington. We haphazardly selected ten, ten, and seven (due to limited sample availability) individuals of *C. anomolus*, *E. ventermaculus*, and *E. pulcher*, respectively, from the Arabian Gulf, and ten individuals each (with the exception of *E. pulcher*, for which we selected eleven individuals) of *C. anomolus*, *E. ventermaculus, A. adenensis*, *E. guttata,* and *H. vulgaris* from the Gulf of Oman. Then, under sterile conditions, we dissected out the entire alimentary tract and removed all other organs (e.g. liver, gonads) under a Zeiss V20 SteREO dissecting microscope using micro-surgery tools. We placed the entire gut into an extraction tube and performed DNA extractions with a DNeasy PowerSoil Pro DNA Isolation Kit (Qiagen, Hilden, Germany). We stored all DNA extracts at 4º C until further processing.

All DNA samples were sent to Jonah Ventures (Boulder, Colorado, USA) for two-step PCRs, library preparation, and sequencing. We targeted two universal gene regions: the mitochondrial cytochrome c oxidase subunit I (COI) for metabarcoding metazoan biodiversity and the chloroplast 23S rRNA for metabarcoding algae. For the COI gene, we selected the m1COIintF forward primer[109] and jgHCO2198 reverse primer[110]. For the 23S gene, we selected the p23SrV_f1 and Diam23Sr1 23S primers[111–113]. All COI and 23S primers contained a 5’ adaptor sequence to facilitate indexing and sequencing. The PCR reactions for both COI and 23S genes were run at a volume of 25 μl according to the Promega PCR Master Mix guidelines (Promega,

Madison, Wisconsin, USA): 12.5 μl Master Mix, 0.5 μM of each primer, 1 μl gDNA, and 10.5 μl DNase/Rnase-free water. For COI, PCR amplification was run with the following conditions: initial denaturation at 94 °C for 2 minutes, followed by 45 cycles of 15 seconds at 94 °C, 30 seconds at 50 °C, and 1 minute at 72 °C, then a final elongation at 72 °C for 10 minutes. For 23S, DNA was PCR-amplified under the following conditions: initial denaturation at 94 °C for 3 minutes, followed by 40 cycles of 30 seconds at 94 °C, 45 seconds at 55 °C, and 1 minute at 72 °C, then a final elongation at 72 °C for 10 minutes. After PCR amplification, each reaction was visually inspected with a 2% agarose gel to ensure successful amplification and determine amplicon size.

All remaining library preparation and sequencing protocols apply to both the COI and 23S markers. Clean-ups were performed by incubating amplicons with Exo1/SAP for 30 minutes at 37 °C, followed by inactivation at 95 °C for 5 minutes, then the products were stored at -20 °C. Next, a second indexing PCR was performed to bind a unique 12-nucleotide index sequence. The PCR reaction included Promega Master mix, 0.5 μM of each primer, and 2 μl of template DNA. The PCR was performed with the following conditions: initial denaturation at 95 °C for 3 minutes, followed by 8 cycles of 95 °C for 30 seconds, 55 °C for 30 seconds, and 72 °C for 30 seconds. Each reaction was visually inspected with a 2% agarose gel to ensure successful amplification.

A volume of 25 μl of each indexed amplicon was cleaned and normalized with the SequalPrep Normalization Kit (Life Technologies, Carlsbad, California, USA) according to the manufacturer's protocol. For sample pooling, 5 μl of each sample was added together. Finally, library pools were sent to the Genohub service provider (Austin, Texas, USA). Prior to sequencing, quality control measures were performed, including

651 bead cleaning with Agencourt AMPure XP beads (Beckman Coulter, Brea, California,
652 USA) to remove <200 bp amplicons, sample quantification with a Qubit Fluorometer
653 (Invitrogen, Carlsbad, California, USA), and amplicon average size analysis with an
654 Agilent TapeStation 4200 (Agilent, Santa Clara, California, USA). Finally, sequencing
655 was performed on an Illumina HiSeq using the HiSeq Rapid SBS Kit v2, 500-cycles
656 (Illumina, San Diego, California, USA).
657
658 *Sequence bioinformatics*
659 For the COI sequences, a joint QIIME[114] and UPARSE[115] pipeline was employed
660 for bioinformatic processing. Sequences were demultiplexed and initial quality filtering
661 was performed with QIIME v1.9.1. Primer sequences were trimmed with Cutadapt
662 v1.18[116], then forward and reverse reads were pair-end merged with USEARCH
663 v11.0.667[117]. Quality filtering was then performed in accordance with the UPARSE
664 pipeline. Sequences were clustered into operational taxonomic units (OTUs) at 99%
665 similarity, and the OTU table was generated by mapping quality-filtered reads back to
666 the OTU seeds. Taxonomy was assigned to OTUs by recording the top basic local
667 alignment search tool (BLASTn[118]) hit when query coverage and percent identity
668 exceeded 95% and 80%, respectively. GenBank was used as the reference database.
669 When OTU taxonomic assignments did not meet these criteria, taxonomy was removed
670 and recorded as “NA.” Finally, we removed all self-hits from the OTU-dataset, which we
671 identified by matching the highest sequence reads of each species to its individuals, as
672 well as unambiguous (>97% identity match) assignments to species not found in the
673 geographic region (specifically *Oncorhynchus nerka*).

For the 23S sequences, raw sequences were processed with the JAMP pipeline (https://github.com/VascoElbrecht/JAMP). After demultiplexing, forward and reverse reads were pair-end merged with USEARCH v11.0.667[117]. Primers were trimmed from both ends using Cutadapt v1.18[116], and quality filtering was conducted with expected error filtering, as implemented through USEARCH[119]. Reads affected by sequencing and PCR error were removed using the UNOISE algorithm[120]. Exact sequence variants (ESVs) were then compiled into an ESV table, which included read counts for each sample. Taxonomy was assigned to each ESV by mapping them against a 23S database from Silva[121], specifying zero deviations to ensure mapping accuracy. Consensus taxonomy was generated from the hit tables, first considering 100% matches, then decreasing by 1% until hits were available for each ESV. Taxonomy that was present in at least 90% of the hits was reported; otherwise, an "NA" was assigned when several different taxa matched the ESV. For error reduction due to misidentified taxa, the bracket was increased to 2% when matches of 97% and higher were present, but no family-level or lower taxonomy was assigned.

Data analyses and modeling

To analyze the community variables, we first calculated the surface area (*SA*) for each sampled outcrop from the curved surface length (*CSL*) by deriving the sampled outcrop's radius *r* ($r = 2*CSL/2\pi$), then computing available surface area under the assumption that outcrops are hemispherical constructs ($SA = 4\pi r_2/2$). We calculated the sum of individuals, species, and their respective body weight for each station to obtain abundance, diversity, and biomass estimates, which we converted to density estimates

by dividing them by the sampled surface area. Using these estimates, we performed three Bayesian hierarchical models, each on the natural logarithm of the response variables (species density, individual density, and biomass per m_2). Models were specified to include the fixed effect of *Location* (*Arabian Gulf vs. Gulf of Oman*) and the random effect of *Site* (*Dhabiya*, *Ras Ghanada*, *Saadiyat*, *Dibba Rock*, *Sharm Rock*, *Snoopy Rock*) and were run with a Gaussian error distribution. For each model, we ran four chains with 4,000 post burn-in samples, and we validated chain convergence visually. We used the default, non-informative priors set by the *brm* function in the *brms* R package[122]. Then, we used the model parameters to predict distributions based on 1,000 draws from the posterior and plotted the distributions, their mean and confidence bands, and the raw data for each site to evaluate model fit.

To examine cryptobenthic fish community composition across the two locations, we created a species-by-sample matrix indicating the abundance of each species in a given sample. We then performed a non-metric multidimensional scaling (nMDS) ordination with the Bray-Curtis dissimilarity matrix of the square-root transformed data in two dimensions (stress = 0.101). We performed a permutational analysis of variance (PERMANOVA) on the same distance matrix (using 999 permutations) and extracted the most influential species using the similarity of percentages (SIMPER) routine. We constructed convex hull polygons for the two locations (as determined by the location of each sample) and plotted them in a biplot with the seven most influential species (average contribution > 2.5%) superimposed. For benthic community composition, we followed a similar process. After our initial categorization, we first combined live coral categories into “branching” and “other” and omitted all categories with fewer than three

records across the entire dataset (bleached coral and hydroids) from the data. We also excluded the “unidentifiable” category (<5% of points). We then calculated the proportional contribution of each category to the benthos in a given sampled outcrop and arranged the data into a sample-by-category matrix and performed another nMDS analysis as per above (with square-root transformed data). We also performed a PERMANOVA and visualized the data in the same way as described above, but we did not perform the SIMPER routine due to the lower number of categories. Further, we scaled the size of the symbols to represent the percent of live coral cover. Finally, we statistically compared live coral cover among the two locations using a Bayesian hierarchical model. We logit-transformed proportional *LiveCoralCover* and specified *Location* as a fixed effect, with *Site* specified as a random effect. Model and chain specifications were programmed as described above.

To compare intrinsic temperature tolerances, as derived from CT_{min} and CT_{max} trials, we ran two separate Bayesian linear models. For both models, we specified an effect of *Population* (i.e., separate levels for each species and their respective Arabian Gulf and Gulf of Oman populations) on the critical thermal limit of individuals and examined differences between pairwise levels using post-hoc contrasts (Tables S3 and S4). We also explored effects of body size on thermal tolerance but found no meaningful effect. Models were run with a Gaussian error distribution and the same specifications as the previous models (e.g., burnin, iterations, priors, etc.). We took 1,000 draws from the posterior parameters to fit posterior distributions as well as their mean and confidence bands and plotted them alongside the raw data. Furthermore, to examine location-specific differences in length-weight relationships and species-specific

abundances, we isolated individuals from three species (*C. anomolus*, *E. pulcher*, and *E. ventermaculus*) and ran separate models for each species to test the effects of total length (*TL*) and *Location* on *Weight*, with log-transformations of both *Weight* and *TL* and the effect of location (with a random effect of *Site*) on abundance. We used a Gaussian error distribution for the first set of models since the data were continuous and approximately normally distributed. We used a negative binomial error distribution for the second set of models since the data were non-negative integers and over-dispersed when run under a Poisson distribution. To validate the model performance, we used the posterior parameters to predict values across a sequence of 100 evenly spaced values within the sampled size range of the two populations. We performed this 500 times and plotted each predicted model fit alongside the raw data. Models were run with the same prior and chain specifications as detailed above.

We examined prey item ingestion of the examined fishes using a network theory approach for both the COI and 23S markers[123]. We first created a presence-absence matrix of OTUs/ESVs across fish individuals in all species and their populations, creating a bipartite dietary network based on prey presence or absence. To examine the community structure within the network, we omitted all prey items with only a single occurrence across the dataset since the full dataset identified the majority of individuals as unique modules. This step reduced the COI dataset from 1,357 to 1,046 unique predator-prey interactions and the 23S dataset from 7,872 to 5,698 predator-prey interactions. We then sought to identify modules within the network using Newman's modularity measure[124]. We used Beckett's community detection algorithm[125], which we re-iterated 20 times for each dataset. We then used the convergent output from the 20

766 iterations to determine the module membership of each individual in our network. We
767 then created a data frame from the original presence-absence matrix that contained
768 each OTU/ESV and its linkage to the fish individual in two columns, which we then
769 summarized by the respective modules. This created a list of symbolic edges in the
770 network across the two columns, linking each prey item to a module, which we plotted
771 as a bipartite dietary network tree using the Fruchterman-Reingold algorithm. We also
772 plotted module membership in a mosaic plot.

773 Furthermore, for the COI and 23S markers, we investigated prey item diversity
774 ingested by each species' population by producing interpolated and extrapolated
775 rarefaction curves, which showcase sequencing depth by plotting prey item species
776 richness by the total number of sequences detected for each species. We ran
777 rarefaction analyses by rarefying species richness estimates for each species or
778 population to an endpoint defined by the maximum sequences in any population using
779 100 bootstraps and 50 knots along the x-axis[126].

780 Finally, we modelled growth and mortality dynamics in cryptobenthic fish
781 assemblages from the two locations, ultimately yielding a standing biomass estimate
782 and three rate-based metrics that serve as indicators of energy and nutrient fluxes, thus
783 indicating ecosystem functioning[21]: produced biomass (in g $d^{-1}m^{-2}$), consumed biomass
784 (in g $d^{-1}m^{-2}$), and total turnover (percent d^{-1})[97,127,128]. Produced biomass represents the
785 amount of fish tissue accumulated by an assemblage (in this case, a cryptobenthic fish
786 assemblage collected in a given sample), thus considering only the growth that will
787 occur on any given day (based on yearly averages in this case). Consumed biomass
788 represents the amount of fish tissue that perished based on our estimates of fish

789 mortality. In this pathway, the energy and nutrients produced by fishes are provided to
790 other consumers or decomposers via predation or detritivory. Finally, total turnover
791 expands on the classic estimate of turnover (the production/standing biomass [P/B]
792 ratio[129]) by also including consumed biomass (consumed biomass/standing biomass)[127].
793 As such, the turnover metric approximates the rate at which particles flow through the
794 system, either via incorporation into fish biomass or release to other consumers through
795 mortality.
796 For the modeling, we first accrued species-specific information on maximum
797 lengths and a range of coarse ecological traits (pertaining to diet, sociality, habitat
798 association, and prevailing mean sea surface temperatures [SST]) from the literature for
799 each species in our samples. We also extracted length-weight relationships at the
800 family-level, since not all species in our samples were common enough to construct
801 robust length-weight relationships. We then used these data to calculate species-
802 specific growth coefficients (K_{max}) to the specified maximum size and modeled individual
803 weight gain based on changes in fish size per day under a Von Bertalanffy Growth
804 Model (VBGM)[128]. By subtracting the observed fish size (as obtained from our samples)
805 from the weight obtained by the same fish after one day (from the model), we calculated
806 the expected biomass production by that individual. We estimated daily mortality rates
807 by calculating species-level mortality risk coefficients via VBGM parameters and
808 SST[127,130], and then we adjusted the risk based on relationships between mortality and
809 body size[131]. Using these coefficients, we obtained a daily survival probability for a
810 given individual in the dataset. By combining this probability with biomass production as
811 obtained from the previous step, we were able to generate the expected loss of biomass

812 due to natural mortality at the individual level. Finally, we summed the individual-level
813 estimates of weight, growth, and mortality for each sample to obtain community-level
814 values of standing biomass, produced biomass, and consumed biomass, which we
815 used to calculate total turnover as the combined quotients of produced and consumed
816 biomass and standing biomass.
817 All data preparation, analyses, and visualizations were performed in *R*[132] (version
818 3.6.1) using the *tidyverse*[133], *vegan*[134], *brms*[122], *iNEXT*[126], *igraph*[135], *bipartite*[136],
819 *tidybayes*[137], *xgboost*[138], *emmeans*[139], *oceanmap*[140], *ncdf4*[141] and *raster*[142] packages.
820 All graphs were made using the *Trimma lantana* and *Coryphaena hippurus* color
821 palettes in the package *fishualize*[143]. Growth modeling was performed using an alpha
822 version of the package *rfishprod*.

References

1. Dornelas, M. *et al.* Assemblage time series reveal biodiversity change but not systematic loss. *Science* **344**, 296–299 (2014).
2. Blowes, S. A. *et al.* The geography of biodiversity change in marine and terrestrial assemblages. *Science* **366**, 339–345 (2019).
3. Mace, G. M., Norris, K. & Fitter, A. H. Biodiversity and ecosystem services: a multilayered relationship. *Trends in ecology & evolution* **27**, 19–26 (2012).
4. Vellend, M. *The theory of ecological communities (MPB-57)*. vol. 75 (Princeton University Press, 2016).
5. Kraft, N. J. *et al.* Community assembly, coexistence and the environmental filtering metaphor. *Functional Ecology* **29**, 592–599 (2015).
6. Leibold, M. A. *et al.* The metacommunity concept: a framework for multi-scale community ecology. *Ecology letters* **7**, 601–613 (2004).
7. Duffy, J. E., Godwin, C. M. & Cardinale, B. J. Biodiversity effects in the wild are common and as strong as key drivers of productivity. *Nature* **549**, 261 (2017).
8. Schweiger, A. K. *et al.* Plant spectral diversity integrates functional and phylogenetic components of biodiversity and predicts ecosystem function. *Nature ecology & evolution* **2**, 976 (2018).
9. Pecl, G. T. *et al.* Biodiversity redistribution under climate change: Impacts on ecosystems and human well-being. *Science* **355**, eaai9214 (2017).
10. Scheffers, B. R. *et al.* The broad footprint of climate change from genes to biomes to people. *Science* **354**, aaf7671 (2016).

11. García, F. C., Bestion, E., Warfield, R. & Yvon-Durocher, G. Changes in temperature alter the relationship between biodiversity and ecosystem functioning. *Proceedings of the National Academy of Sciences* **115**, 10989–10994 (2018).
12. Pörtner, H. O. & Farrell, A. P. Physiology and climate change. *Science* **322**, 690–692 (2008).
13. Deutsch, C., Ferrel, A., Seibel, B., Pörtner, H.-O. & Huey, R. B. Climate change tightens a metabolic constraint on marine habitats. *Science* **348**, 1132–1135 (2015).
14. Bozinovic, F. & Pörtner, H. Physiological ecology meets climate change. *Ecology and evolution* **5**, 1025–1030 (2015).
15. Barneche, D. R., Jahn, M. & Seebacher, F. Warming increases the cost of growth in a model vertebrate. *Functional Ecology* (2019).
16. Brown, J. H., Hall, C. A. & Sibly, R. M. Equal fitness paradigm explained by a trade-off between generation time and energy production rate. *Nature ecology & evolution* **2**, 262 (2018).
17. Toseland, A. *et al.* The impact of temperature on marine phytoplankton resource allocation and metabolism. *Nature Climate Change* **3**, 979 (2013).
18. Barneche, D. R. & Allen, A. P. The energetics of fish growth and how it constrains food-web trophic structure. *Ecology letters* **21**, 836–844 (2018).
19. Chesson, P. Mechanisms of maintenance of species diversity. *Annual review of Ecology and Systematics* **31**, 343–366 (2000).
20. Barnes, A. D. *et al.* Energy flux: the link between multitrophic biodiversity and ecosystem functioning. *Trends in ecology & evolution* **33**, 186–197 (2018).
21. Brandl, S. J. *et al.* Coral reef ecosystem functioning: eight core processes and the role of biodiversity. *Frontiers in Ecology and the Environment* (2019).

22. Spalding, M. *et al.* Mapping the global value and distribution of coral reef tourism. *Marine Policy* **82**, 104–113 (2017).
23. Hughes, T. P. *et al.* Spatial and temporal patterns of mass bleaching of corals in the Anthropocene. *Science* **359**, 80–83 (2018).
24. Pratchett, M. S., Hoey, A. S., Wilson, S. K., Messmer, V. & Graham, N. A. Changes in biodiversity and functioning of reef fish assemblages following coral bleaching and coral loss. *Diversity* **3**, 424–452 (2011).
25. Brandl, S. J., Emslie, M. J. & Ceccarelli, D. M. Habitat degradation increases functional originality in highly diverse coral reef fish assemblages. *Ecosphere* **7**, (2016).
26. Fontoura, L. *et al.* Climate-driven shift in coral morphological structure predicts decline of juvenile reef fishes. *Global change biology* (2019).
27. Bellwood, D. R., Hoey, A. S., Ackerman, J. L. & Depczynski, M. Coral bleaching, reef fish community phase shifts and the resilience of coral reefs. *Global Change Biology* **12**, 1587–1594 (2006).
28. Robinson, J. P. *et al.* Productive instability of coral reef fisheries after climate-driven regime shifts. *Nature ecology & evolution* **3**, 183 (2019).
29. Wismer, S., Tebbett, S. B., Streit, R. P. & Bellwood, D. R. Young fishes persist despite coral loss on the Great Barrier Reef. *Communications Biology* **2**, 456 (2019).
30. Taylor, B. M. *et al.* Synchronous biological feedbacks in parrotfishes associated with pantropical coral bleaching. *Global Change Biology* (2019).
31. Morais, R. A. *et al.* Severe coral loss shifts energetic dynamics on a coral reef. *Functional Ecology* (2020).

32. Pörtner, H. O. & Knust, R. Climate change affects marine fishes through the oxygen limitation of thermal tolerance. *science* **315**, 95–97 (2007).

33. Comte, L. & Olden, J. D. Climatic vulnerability of the world's freshwater and marine fishes. *Nature Climate Change* **7**, 718 (2017).

34. Munday, P. L., McCormick, M. I. & Nilsson, G. E. Impact of global warming and rising CO2 levels on coral reef fishes: what hope for the future? *Journal of Experimental Biology* **215**, 3865–3873 (2012).

35. Munday, P. L., Jones, G. P., Pratchett, M. S. & Williams, A. J. Climate change and the future for coral reef fishes. *Fish and Fisheries* **9**, 261–285 (2008).

36. Donelson, J., Munday, P., McCormick, M. & Pitcher, C. Rapid transgenerational acclimation of a tropical reef fish to climate change. *Nature Climate Change* **2**, 30 (2012).

37. Ern, R., Huong, D., Cong, N., Bayley, M. & Wang, T. Effect of salinity on oxygen consumption in fishes: a review. *Journal of Fish Biology* **84**, 1210–1220 (2014).

38. Johansen, J. & Jones, G. Increasing ocean temperature reduces the metabolic performance and swimming ability of coral reef damselfishes. *Global Change Biology* **17**, 2971–2979 (2011).

39. Rummer, J. L. *et al.* Life on the edge: thermal optima for aerobic scope of equatorial reef fishes are close to current day temperatures. *Global change biology* **20**, 1055–1066 (2014).

40. Nilsson, G. E., Crawley, N., Lunde, I. G. & Munday, P. L. Elevated temperature reduces the respiratory scope of coral reef fishes. *Global Change Biology* **15**, 1405–1412 (2009).

41. Eme, J. & Bennett, W. A. Critical thermal tolerance polygons of tropical marine fishes from Sulawesi, Indonesia. *Journal of Thermal Biology* **34**, 220–225 (2009).

912 42. Gardiner, N. M., Munday, P. L. & Nilsson, G. E. Counter-gradient variation in respiratory
913 performance of coral reef fishes at elevated temperatures. *PLoS One* **5**, e13299 (2010).
914 43. Bernal, M. A. *et al.* Species-specific molecular responses of wild coral reef fishes during a
915 marine heatwave. *Science advances* **6**, eaay3423 (2020).
916 44. Mora, C. & Ospina, A. Tolerance to high temperatures and potential impact of sea warming
917 on reef fishes of Gorgona Island (tropical eastern Pacific). *Marine Biology* **139**, 765–769
918 (2001).
919 45. Feary, D. A. *et al.* Latitudinal shifts in coral reef fishes: why some species do and others do
920 not shift. *Fish and Fisheries* **15**, 593–615 (2014).
921 46. Bernal, M. A. *et al.* Phenotypic and molecular consequences of stepwise temperature
922 increase across generations in a coral reef fish. *Molecular Ecology* **27**, 4516–4528 (2018).
923 47. Grenchik, M., Donelson, J. & Munday, P. Evidence for developmental thermal acclimation
924 in the damselfish, Pomacentrus moluccensis. *Coral Reefs* **32**, 85–90 (2013).
925 48. Miller, D. D., Ota, Y., Sumaila, U. R., Cisneros-Montemayor, A. M. & Cheung, W. W.
926 Adaptation strategies to climate change in marine systems. *Global change biology* **24**, e1–
927 e14 (2018).
928 49. Brandl, S. J., Goatley, C. H., Bellwood, D. R. & Tornabene, L. The hidden half: ecology and
929 evolution of cryptobenthic fishes on coral reefs. *Biological Reviews* **93**, 1846–1873 (2018).
930 50. Brandl, S. J., Casey, J. M., Knowlton, N. & Duffy, J. E. Marine dock pilings foster diverse,
931 native cryptobenthic fish assemblages across bioregions. *Ecology and evolution* **7**, 7069–
932 7079 (2017).

51. Ahmadia, G. N., Tornabene, L., Smith, D. J. & Pezold, F. L. The relative importance of regional, local, and evolutionary factors structuring cryptobenthic coral-reef assemblages. *Coral Reefs* **37**, 279–293 (2018).
52. Coker, D. J., DiBattista, J. D., Sinclair-Taylor, T. H. & Berumen, M. L. Spatial patterns of cryptobenthic coral-reef fishes in the Red Sea. *Coral Reefs* 1–7 (2017).
53. Brandl, S. J. *et al.* Demographic dynamics of the smallest marine vertebrates fuel coral reef ecosystem functioning. *Science* **364**, 1189–1192 (2019).
54. Miller, P. J. Miniature vertebrates. The implications of small body size. in vol. 69 (Oxford University Press, 1996).
55. Depczynski, M. & Bellwood, D. Microhabitat utilisation patterns in cryptobenthic coral reef fish communities. *Marine Biology* **145**, 455–463 (2004).
56. Bellwood, D. R. *et al.* Coral recovery may not herald the return of fishes on damaged coral reefs. *Oecologia* **170**, 567–573 (2012).
57. Depczynski, M. & Bellwood, D. R. Shortest recorded vertebrate lifespan found in a coral reef fish. *Current Biology* **15**, R288–R289.
58. Tornabene, L., Valdez, S., Erdmann, M. & Pezold, F. Support for a 'Center of Origin'in the Coral Triangle: Cryptic diversity, recent speciation, and local endemism in a diverse lineage of reef fishes (Gobiidae: Eviota). *Molecular phylogenetics and evolution* **82**, 200–210 (2015).
59. Howells, E. J. *et al.* Corals in the hottest reefs in the world exhibit symbiont fidelity not flexibility. *Molecular Ecology* **29**, 899–911 (2020).

60. Howells, E. J., Abrego, D., Meyer, E., Kirk, N. L. & Burt, J. A. Host adaptation and unexpected symbiont partners enable reef-building corals to tolerate extreme temperatures. *Global change biology* **22**, 2702–2714 (2016).
61. Riegl, B. M. & Purkis, S. J. Coral reefs of the Gulf: adaptation to climatic extremes in the world's hottest sea. in *Coral reefs of the Gulf* 1–4 (Springer, 2012).
62. Purkis, S. J. & Riegl, B. M. Geomorphology and Reef Building in the SE Gulf. in *Coral Reefs of the Gulf: Adaptation to Climatic Extremes* (eds. Riegl, B. M. & Purkis, S. J.) 33–50 (Springer Netherlands, 2012). doi:10.1007/978-94-007-3008-3_3.
63. Price, A., Sheppard, C. & Roberts, C. The Gulf: its biological setting. *Marine Pollution Bulletin* **27**, 9–15 (1993).
64. Eagderi, S., Fricke, R., Esmaeili, H. & Jalili, P. Annotated checklist of the fishes of the Persian Gulf: Diversity and conservation status. *Iranian Journal of Ichthyology* **6**, 1–171 (2019).
65. Casey, J. M. *et al.* Reconstructing hyperdiverse food webs: Gut content metabarcoding as a tool to disentangle trophic interactions on coral reefs. *Methods in Ecology and Evolution* **10**, 1157–1170 (2019).
66. Depczynski, M. & Bellwood, D. R. The role of cryptobenthic reef fishes in coral reef trophodynamics. *Marine Ecology Progress Series* **256**, 183–191 (2003).
67. Pratchett, M. S., Wilson, S. K. & Munday, P. L. 13 Effects of climate change on coral reef fishes. *Ecology of fishes on coral reefs* 127 (2015).
68. Krupp, F. & Müller, T. The status of fish populations in the northern Arabian Gulf two years after the 1991 Gulf War oil spill. *Courier Forschungsinst Senckenb* **166**, 67–75 (1994).

69. Bishop, J. History and current checklist of Kuwait's ichthyofauna. *Journal of Arid Environments* **54**, 237–256 (2003).
70. Feary, D. A., Burt, J. A., Cavalcante, G. H. & Bauman, A. G. Extreme Physical Factors and the Structure of Gulf Fish and Reef Communities. in *Coral Reefs of the Gulf: Adaptation to Climatic Extremes* (eds. Riegl, B. M. & Purkis, S. J.) 163–170 (Springer Netherlands, 2012). doi:10.1007/978-94-007-3008-3_9.
71. Donelson, J. M., Munday, P. L., McCORMICK, M. I. & Nilsson, G. E. Acclimation to predicted ocean warming through developmental plasticity in a tropical reef fish. *Global Change Biology* **17**, 1712–1719 (2011).
72. Ohlberger, J. Climate warming and ectotherm body size–from individual physiology to community ecology. *Functional Ecology* **27**, 991–1001 (2013).
73. Gardner, J. L., Peters, A., Kearney, M. R., Joseph, L. & Heinsohn, R. Declining body size: a third universal response to warming? *Trends in ecology & evolution* **26**, 285–291 (2011).
74. Peig, J. & Green, A. J. The paradigm of body condition: a critical reappraisal of current methods based on mass and length. *Functional Ecology* **24**, 1323–1332 (2010).
75. Sullam, K. E. *et al.* Changes in digestive traits and body nutritional composition accommodate a trophic niche shift in Trinidadian guppies. *Oecologia* **177**, 245–257 (2015).
76. Whelan, C. J., Brown, J. S., Schmidt, K. A., Steele, B. B. & Willson, M. F. Linking consumer–resource theory and digestive physiology: application to diet shifts. *Evolutionary Ecology Research* **2**, 911–934 (2000).
77. Petchey, O. L. Prey diversity, prey composition, and predator population dynamics in experimental microcosms. *Journal of Animal Ecology* **69**, 874–882 (2000).

998 78. Merrick, R. L., Chumbley, M. K. & Byrd, G. V. Diet diversity of Steller sea lions
999 (Eumetopias jubatus) and their population decline in Alaska: a potential relationship. *Can. J.*
1000 *Fish. Aquat. Sci.* **54**, 1342–1348 (1997).
1001 79. Hondorp, D. W., Pothoven, S. A. & Brandt, S. B. Influence of Diporeia density on diet
1002 composition, relative abundance, and energy density of planktivorous fishes in southeast
1003 Lake Michigan. *Transactions of the American fisheries Society* **134**, 588–601 (2005).
1004 80. Shraim, R. *et al.* Environmental Extremes Are Associated with Dietary Patterns in Arabian
1005 Gulf Reef Fishes. *Frontiers in Marine Science* **4**, 285 (2017).
1006 81. Agorreta, A. *et al.* Molecular phylogenetics of Gobioidei and phylogenetic placement of
1007 European gobies. *Molecular Phylogenetics and Evolution* **69**, 619–633 (2013).
1008 82. Thacker, C. E. & Roje, D. M. Phylogeny of Gobiidae and identification of gobiid lineages.
1009 *Systematics and Biodiversity* **9**, 329–347 (2011).
1010 83. Kovačić, M., Bogorodsky, S. V. & Mal, A. O. Two new species of Coryogalops
1011 (Perciformes: Gobiidae) from the Red Sea. *Zootaxa* **3881**, 513–531 (2014).
1012 84. Rishworth GM, Strydom NA & Perissinotto R. Fishes associated with living stromatolite
1013 communities in peritidal pools: predators, recruits and ecological traps. *Mar Ecol Prog Ser*
1014 **580**, 153–167 (2017).
1015 85. Munday, P. L. & Jones, G. P. The ecological implications of small body size among coral-
1016 reef fishes. *Oceanogr Mar Biol Annu Rev* **36**, 373–411 (1998).
1017 86. Sandblom, E. *et al.* Physiological constraints to climate warming in fish follow principles of
1018 plastic floors and concrete ceilings. *Nature communications* **7**, 11447 (2016).

87. Norin, T. & Metcalfe, N. B. Ecological and evolutionary consequences of metabolic rate plasticity in response to environmental change. *Philosophical Transactions of the Royal Society B* **374**, 20180180 (2019).
88. Sheldon, K. S., Yang, S. & Tewksbury, J. J. Climate change and community disassembly: impacts of warming on tropical and temperate montane community structure. *Ecology Letters* **14**, 1191–1200 (2011).
89. Crossland, C., Hatcher, B. & Smith, S. Role of coral reefs in global ocean production. *Coral reefs* **10**, 55–64 (1991).
90. Gove, J. M. *et al.* Near-island biological hotspots in barren ocean basins. *Nature communications* **7**, 10581 (2016).
91. De Goeij, J. M. *et al.* Surviving in a marine desert: the sponge loop retains resources within coral reefs. *Science* **342**, 108–110 (2013).
92. Wild, C. *et al.* Coral mucus functions as an energy carrier and particle trap in the reef ecosystem. *Nature* **428**, 66–70 (2004).
93. Hamner, W., Jones, M., Carleton, J., Hauri, I. & Williams, D. M. Zooplankton, planktivorous fish, and water currents on a windward reef face: Great Barrier Reef, Australia. *Bulletin of Marine Science* **42**, 459–479 (1988).
94. Hatcher, B. G. Coral reef primary productivity: a beggar's banquet. *Trends in Ecology & Evolution* **3**, 106–111 (1988).
95. Bacon, P., Gurney, W., Jones, W., McLaren, I. & Youngson, A. Seasonal growth patterns of wild juvenile fish: partitioning variation among explanatory variables, based on individual growth trajectories of Atlantic salmon (Salmo salar) parr. *Journal of Animal Ecology* **74**, 1–11 (2005).

96. Coles, S. L. Coral species diversity and environmental factors in the Arabian Gulf and the Gulf of Oman: a comparison to the Indo-Pacific region. *Atoll Research Bulletin* (2003).

97. Morais, R. A. & Bellwood, D. R. Pelagic Subsidies Underpin Fish Productivity on a Degraded Coral Reef. *Current Biology* **29**, 1521–1527 (2019).

98. Riegl, B. Effects of the 1996 and 1998 positive sea-surface temperature anomalies on corals, coral diseases and fish in the Arabian Gulf (Dubai, UAE). *Marine biology* **140**, 29–40 (2002).

99. Riegl, B. & Purkis, S. Coral population dynamics across consecutive mass mortality events. *Global change biology* **21**, 3995–4005 (2015).

100. Burt, J., Al-Harthi, S. & Al-Cibahy, A. Long-term impacts of coral bleaching events on the world's warmest reefs. *Marine environmental research* **72**, 225–229 (2011).

101. Burt, J. A., Paparella, F., Al-Mansoori, N., Al-Mansoori, A. & Al-Jailani, H. Causes and consequences of the 2017 coral bleaching event in the southern Persian/Arabian Gulf. *Coral Reefs* **38**, 567–589 (2019).

102. Coker, D. J., Wilson, S. K. & Pratchett, M. S. Importance of live coral habitat for reef fishes. *Reviews in Fish Biology and Fisheries* **24**, 89–126 (2014).

103. Pratchett, M. S., Baird, A. H., Bauman, A. G. & Burt, J. A. Abundance and composition of juvenile corals reveals divergent trajectories for coral assemblages across the United Arab Emirates. *Marine Pollution Bulletin* **114**, 1031–1035 (2017).

104. Munday, P. L. Habitat loss, resource specialization, and extinction on coral reefs. *Global Change Biology* **10**, 1642–1647 (2004).

105. Burt, J. A. *et al.* Biogeographic patterns of reef fish community structure in the northeastern Arabian Peninsula. *ICES Journal of Marine Science* **68**, 1875–1883 (2011).

106. Brose, U. *et al.* Predator traits determine food-web architecture across ecosystems. *Nature ecology & evolution* **3**, 919 (2019).

107. Ackerman, J. L. & Bellwood, D. R. Reef fish assemblages: a re-evaluation using enclosed rotenone stations. *Marine Ecology-Progress Series* **206**, 227–237 (2000).

108. Beitinger, T. L., Bennett, W. A. & McCauley, R. W. Temperature tolerances of North American freshwater fishes exposed to dynamic changes in temperature. *Environmental biology of fishes* **58**, 237–275 (2000).

109. Leray, M. *et al.* A new versatile primer set targeting a short fragment of the mitochondrial COI region for metabarcoding metazoan diversity: application for characterizing coral reef fish gut contents. *Frontiers in zoology* **10**, 34 (2013).

110. Geller, J., Meyer, C., Parker, M. & Hawk, H. Redesign of PCR primers for mitochondrial cytochrome c oxidase subunit I for marine invertebrates and application in all-taxa biotic surveys. *Molecular ecology resources* **13**, 851–861 (2013).

111. Sherwood, A. R. & Presting, G. G. Universal primers amplify a 23S rDNA plastid marker in eukaryotic algae and cyanobacteria. *Journal of phycology* **43**, 605–608 (2007).

112. Hamsher, S. E., Evans, K. M., Mann, D. G., Poulíčková, A. & Saunders, G. W. Barcoding diatoms: exploring alternatives to COI-5P. *Protist* **162**, 405–422 (2011).

113. Cannon, M. *et al.* In silico assessment of primers for eDNA studies using PrimerTree and application to characterize the biodiversity surrounding the Cuyahoga River. *Scientific reports* **6**, 22908 (2016).

114. Caporaso, J. G. *et al.* QIIME allows analysis of high-throughput community sequencing data. *Nature methods* **7**, 335 (2010).

115. Edgar, R. C. UPARSE: highly accurate OTU sequences from microbial amplicon reads. *Nature methods* **10**, 996 (2013).

116. Martin, M. Cutadapt removes adapter sequences from high-throughput sequencing reads. *EMBnet. journal* **17**, 10–12 (2011).

117. Edgar, R. C. Search and clustering orders of magnitude faster than BLAST. *Bioinformatics* **26**, 2460–2461 (2010).

118. Camacho, C. *et al.* BLAST+: architecture and applications. *BMC bioinformatics* **10**, 421 (2009).

119. Edgar, R. C. & Flyvbjerg, H. Error filtering, pair assembly and error correction for next-generation sequencing reads. *Bioinformatics* **31**, 3476–3482 (2015).

120. Edgar, R. C. UNOISE2: improved error-correction for Illumina 16S and ITS amplicon sequencing. *BioRxiv* 081257 (2016).

121. Yilmaz, P. *et al.* The SILVA and "all-species living tree project (LTP)" taxonomic frameworks. *Nucleic acids research* **42**, D643–D648 (2013).

122. Bürkner, P.-C. Advanced Bayesian Multilevel Modeling with the R Package brms. *arXiv preprint arXiv:1705.11123* (2017).

123. Wasserman, S. & Faust, K. *Social network analysis: Methods and applications*. vol. 8 (Cambridge university press, 1994).

124. Newman, M. E. Modularity and community structure in networks. *Proceedings of the national academy of sciences* **103**, 8577–8582 (2006).

125. Beckett, S. J. Improved community detection in weighted bipartite networks. *Royal Society open science* **3**, 140536 (2016).

126. Hsieh, T., Ma, K. & Chao, A. iNEXT: an R package for rarefaction and extrapolation of species diversity (Hill numbers). *Methods in Ecology and Evolution* (2016).

127. Brandl, S. J. *et al.* Supplemental Materials for Demographic dynamics of the smallest marine vertebrates fuel coral reef ecosystem functioning. *Science* **364**, 1189–1192 (2019).

128. Morais, R. A. & Bellwood, D. R. Global drivers of reef fish growth. *Fish and Fisheries*.

129. Allen, K. R. Relation between production and biomass. *Journal of the Fisheries Board of Canada* **28**, 1573–1581 (1971).

130. Pauly, D. On the interrelationships between natural mortality, growth parameters, and mean environmental temperature in 175 fish stocks. *ICES Journal of Marine Science* **39**, 175–192 (1980).

131. Gislason, H., Daan, N., Rice, J. C. & Pope, J. G. Size, growth, temperature and the natural mortality of marine fish. *Fish and Fisheries* **11**, 149–158 (2010).

132. R Core Team. *R: A language and environment for statistical computing.* (2019).

133. Wickham, H. Tidyverse: Easily install and load'tidyverse'packages. *R package version* **1**, (2017).

134. Oksanen, J. *et al.* The vegan package. *Community ecology package* **10**, (2007).

135. Csardi, G. & Nepusz, T. The igraph software package for complex network research. *InterJournal, Complex Systems* **1695**, 1–9 (2006).

136. Dormann, C. F., Gruber, B. & Fründ, J. Introducing the bipartite package: analysing ecological networks. *interaction* **1**, (2008).

137. Kay, M. tidybayes: Tidy data and geoms for Bayesian models. *R package version* **1**, (2018).

138. Chen, T., He, T., Benesty, M., Khotilovich, V. & Tang, Y. Xgboost: extreme gradient boosting. *R package version 0.4-2* 1–4 (2015).

139. Lenth, R., Singmann, H., Love, J., Buerkner, P. & Herve, M. Package "emmeans": Estimated marginal means, aka least-squares means. *Compr. R Arch. Netw* 1–67 (2019).

140. Bauer, R. Oceanmap: a plotting toolbox for 2D oceanographic data. *R package, version 0.0* **9**, (2017).

141. Pierce, D. & Pierce, M. D. Package 'ncdf4'. (2019).

142. Hijmans, R. J. *et al.* Raster package in R. (2013).

143. Schiettekatte, N. M., Brandl, S. J. & Casey, J. M. *fishualize: Color palettes based on fish species*. (2019).

144. Morgan, R., Finnøen, M. H. & Jutfelt, F. CT max is repeatable and doesn't reduce growth in zebrafish. *Scientific reports* **8**, 7099 (2018).

Acknowledgments

We thank the Environment Agency Abu Dhabi (TMBS/18/L/179) and Dibba Municipality (unnumbered) for collection permits and the UAE Ministry of Environment and Climate Change for the tissue export permit (AUD-Q-22-1110520). All work was performed under NYUAD IACUC approval 18-0003. We further thank the NYU Abu Dhabi Center for Genomics and Systems Biology for sequencing funding and the NYU Abu Dhabi Core Facilities group for support of field collections and thermal experiments. We thank D McParland and G Vaughan for field support, N Al-Mansoori for assistance with processing specimens in the laboratory, and K Maslenikov and J Huie for assistance in cataloging specimens at the University of Washington. Partial fieldwork funding was provided to L Tornabene by the University of Washington. We thank Dr. A McKay and three anonymous reviewers for their feedback on our manuscript.

Author contributions

SJB and JLJ designed the study; SJB, JLJ, JMC, and LT performed field collections; JLJ ran physiological trials; SJB, JMC, and LT performed laboratory work; JAB and LT provided funding and resources; SJB performed data analysis and visualization; SJB and RAM performed population modeling; SJB wrote the first draft of the manuscript, and all authors contributed to writing thereafter.

Data accessibility and conflicts of interest

All data and code necessary to produce the results are included in this submission and will be made public upon publication of the paper. We declare no conflict of interest.

Supplemental Material

Table S1 | Seasonal temperature profiles derived from *in situ* data loggers deployed at various periods at the sample sites. Maximum, minimum, and mean values are daily estimates. Seasons were defined as: spring = March 1st to May 31st; summer = June 1st to August 31st; fall = September 1st to November 30th; winter = December 1st to February 28th.

Location	Year	Season	Maximum	Minimum	Mean
Arabian Gulf	2012	fall	35.58	24.73	30.89
Arabian Gulf	2012	spring	32.79	27.24	30.80
Arabian Gulf	2012	summer	35.99	30.77	33.94
Arabian Gulf	2012	winter	26.52	21.10	24.11
Arabian Gulf	2013	fall	34.89	23.86	30.38
Arabian Gulf	2013	spring	31.89	22.25	26.30
Arabian Gulf	2013	summer	35.53	28.89	33.17
Arabian Gulf	2013	winter	28.89	17.32	22.36
Arabian Gulf	2014	fall	34.84	24.27	30.68
Arabian Gulf	2014	spring	33.47	21.18	27.12
Arabian Gulf	2014	summer	35.80	30.60	33.68
Arabian Gulf	2014	winter	25.40	18.65	21.25
Arabian Gulf	2015	fall	35.77	23.33	30.66
Arabian Gulf	2015	spring	32.46	20.53	26.67
Arabian Gulf	2015	summer	35.80	31.48	33.87
Arabian Gulf	2015	winter	25.99	19.34	22.33
Arabian Gulf	2016	fall	34.68	19.03	32.06
Arabian Gulf	2016	spring	32.05	22.23	25.44
Arabian Gulf	2016	summer	35.34	30.57	33.65
Arabian Gulf	2016	winter	23.28	19.20	21.25
Gulf of Oman	2012	fall	31.89	25.43	29.01
Gulf of Oman	2012	summer	34.78	23.55	29.96
Gulf of Oman	2012	winter	26.48	23.50	25.15
Gulf of Oman	2013	fall	32.64	24.27	29.31
Gulf of Oman	2013	spring	31.05	22.54	25.78
Gulf of Oman	2013	summer	33.05	24.22	29.08
Gulf of Oman	2013	winter	26.65	22.06	24.26
Gulf of Oman	2014	fall	32.90	25.02	29.83
Gulf of Oman	2014	spring	33.08	21.72	25.85
Gulf of Oman	2014	summer	33.94	24.24	30.75
Gulf of Oman	2014	winter	24.97	21.49	22.85

Table S2 | Presence, abundance, and previous records of species sampled in the present study. Each row represents a species, with columns *AG* (Arabian Gulf) and *GO* (Gulf of Oman) indicating the abundance of the species in our samples. Column *R* indicates whether the species has been previously recorded in other parts of the Arabian Gulf (* = yes, – = no). References for previous records are provided.

Family	***Species***	***AG***	***GO***	***R***	***Reference***
Apogonidae	*Apogon coccineus*	6	10	*	present
Apogonidae	*Apogonichthyoides taeniatus*	2	0	*	present
Apogonidae	*Cheilodipterus novemstriatus*	2	9	*	present
Apogonidae	*Cheilodipterus persicus*	0	1	*	Krupp & Müller 1994
Apogonidae	*Fowleria variegata*	5	1	*	present
Apogonidae	*Ostorhinchus cyanosoma*	0	15	*	Krupp & Müller 1994
Apogonidae	*Ostorhinchus fleurieu*	0	30	*	Eagderi et al. 2019
Batrachoididae	*Colletteichthys occidentalis*	6	0	*	present
Blenniidae	*Antennablennius adenensis*	0	54	*	Bishop 2003
Blenniidae	*Ecsenius pulcher*	8	97	*	present
Blenniidae	*Laiphognathus multimaculatus*	1	0	*	present
Bythitidae	*Dinematichthys iluocoeteoides*	5	0	*	present
Gobiidae	*Asterropteryx semipunctata*	0	2	*	Krupp & Müller 1994
Gobiidae	*Callogobius bifasciatus*	2	0	*	present
Gobiidae	*Callogobius speA*	0	3	*	Eagderi et al. 2019
Gobiidae	*Coryogalops anomalus*	65	33	*	present
Gobiidae	*Eviota guttata*	0	69	*	Krupp & Müller 1994
Gobiidae	*Eviota punyit*	0	12	*	Krupp & Müller 1994[1]
Gobiidae	*Favonigobius melanobranchus*	1	0	*	present
Gobiidae	*Fusigobius inframaculatus*	0	3	*	Eagderi et al. 2019
Gobiidae	*Gnatholepis caudimaculata*	0	14	*	Eagderi et al. 2019
Gobiidae	*Gobiodon reticulatus*	0	2	*	Bishop 2003
Gobiidae	*Hetereleotris vulgaris*	0	405	*	Eagderi et al. 2019
Gobiidae	*Istigobius decoratus*	0	15	*	Eagderi et al. 2019
Gobiidae	*Priolepis cincta*	0	4	*	Winterbottom & Burridge 1992
Gobiidae	*Priolepis randalli*	0	2	*	Winterbottom & Burridge 1993
Gobiidae	*Priolepis semidoliata*	0	10	–	NA
Gobiidae	*Trimma corallinum*	0	11	*	Eagderi et al. 2019[2]
Muraenidae	*Gymnothorax speA*	0	12	*	Eagderi et al. 2019[3]
Ostraciidae	*Ostracion cubicus*	0	3	*	Eagderi et al. 2019
Pomacanthidae	*Pomacanthus maculosus*	7	0	*	present
Pomacentridae	*Chromis flavaxilla*	0	19	*	Bishop 2003
Pomacentridae	*Chromis xanthopterygius*	0	3	*	Bishop 2003
Pomacentridae	*Neopomacentrus cyanomos*	0	38	*	Bishop 2003
Pomacentridae	*Neopomacentrus miryae*	0	38	–	NA
Pomacentridae	*Neopomacentrus sindensis*	0	6	*	Bishop 2003
Pomacentridae	*Pomacentrus aquilus*	3	0	*	present
Pomacentridae	*Pomacentrus leptus*	0	5	*	Bishop 2003
Pomacentridae	*Pomacentrus trichrourus*	5	0	*	present
Pseudochromidae	*Pseudochromis aldabraensis*	0	4	*	Bishop 2003
Pseudochromidae	*Pseudochromis linda*	1	0	*	present
Pseudochromidae	*Pseudochromis nigrovittatus*	2	1	*	present

Pseudochromidae	*Pseudochromis persicus*	1	0	*	present
Serranidae	*Cephalopholis hemistiktos*	2	2	*	present
Syngnathidae	*Corythoichthys flavofasciata*	0	5	*	Froese & Pauly 2019
Syngnathidae	*Doryrhamphus excisus*	0	3	*	Bishop 2003
Tripterygiidae	*Enneapterygius ventermaculus*	131	262	*	present
Tripterygiidae	*Helcogramma fuscopinna*	0	134	–	NA

[1]identified as *E. sebreei*
[2]synonymous with *T. winterbottomi*
[3]genus level

Table S3 | Contrasts between levels of the explanatory variable for the model testing CT_{max} differences in cryptobenthic reef fishes. Population columns highlight the contrast estimated in the model, whereas the estimate and its confidence intervals indicate estimated differences.

Population I	Population II	Estimate	LCI	UCI
C. anomolus.AG	*E. pulcher.AG*	*0.486*	*-0.079*	*1.054*
C. anomolus.AG	*E. ventermaculus.AG*	*1.360*	*0.808*	*1.949*
C. anomolus.AG	*E. pulcher.GoO*	*1.114*	*0.581*	*1.726*
C. anomolus.AG	*E. ventermaculus.GoO*	*1.633*	*0.939*	*2.342*
C. anomolus.AG	*E. guttata.GoO*	*1.143*	*0.534*	*1.759*
C. anomolus.AG	*H. fuscopinna.GoO*	*2.392*	*1.758*	*2.992*
C. anomolus.AG	*H. vulgaris.GoO*	*0.492*	*-0.061*	*1.078*
E. pulcher.AG	*E. ventermaculus.AG*	*0.879*	*0.509*	*1.252*
E. pulcher.AG	*E. pulcher.GoO*	*0.636*	*0.244*	*1.016*
E. pulcher.AG	*E. ventermaculus.GoO*	*1.159*	*0.624*	*1.737*
E. pulcher.AG	*E. guttata.GoO*	*0.656*	*0.227*	*1.134*
E. pulcher.AG	*H. fuscoguttata.GoO*	*1.905*	*1.463*	*2.341*
E. pulcher.AG	*H. vulgaris.GoO*	*0.011*	*-0.368*	*0.417*
E. ventermaculus.AG	*E. pulcher.GoO*	*-0.245*	*-0.640*	*0.118*
E. ventermaculus.AG	*E. ventermaculus.GoO*	*0.277*	*-0.260*	*0.815*
E. ventermaculus.AG	*E. guttata.GoO*	*-0.225*	*-0.680*	*0.212*
E. ventermaculus.AG	*H. fuscopinna.GoO*	*1.024*	*0.578*	*1.449*
E. ventermaculus.AG	*H. vulgaris.GoO*	*-0.878*	*-1.265*	*-0.508*
E. pulcher.GoO	*E. ventermaculus.GoO*	*0.519*	*-0.0290*	*1.073*
E. pulcher.GoO	*E. guttata.GoO*	*0.020*	*-0.426*	*0.494*
E. pulcher.GoO	*H. fuscopinna.GoO*	*1.274*	*0.839*	*1.726*
E. pulcher.GoO	*H. vulgaris.GoO*	*-0.628*	*-1.037*	*-0.253*
E. ventermaculus.GoO	*E. guttata.GoO*	*-0.502*	*-1.125*	*0.106*
E. ventermaculus.GoO	*H. fuscopinna.GoO*	*0.750*	*0.130*	*1.344*
E. ventermaculus.GoO	*H. vulgaris.GoO*	*-1.148*	*-1.710*	*-0.584*
E. guttata.GoO	*H. fuscopinna.GoO*	*1.252*	*0.735*	*1.778*
E. guttata.GoO	*H. vulgaris.GoO*	*-0.647*	*-1.094*	*-0.148*
H. fuscopinna.GoO	*H. vulgaris.GoO*	*-1.906*	*-2.363*	*-1.449*

Table S4 | Contrasts between levels of the explanatory variable for the model testing CT_{min} differences in cryptobenthic reef fishes. Population columns highlight the contrast estimated in the model, whereas the estimate and its confidence intervals indicate estimated differences.

Population I	Population II	Estimate	LCI	UCI
C. anomolus.AG	*E. pulcher.AG*	*0.613*	*0.173*	*1.069*
C. anomolus.AG	*E. ventermaculus.AG*	*-0.400*	*-0.851*	*0.054*
C. anomolus.AG	*E. pulcher.GoO*	*0.747*	*0.316*	*1.211*
C. anomolus.AG	*E. ventermaculus.GoO*	*-1.391*	*-1.887*	*-0.888*
C. anomolus.AG	*E. guttata.GoO*	*-0.784*	*-1.241*	*-0.317*
C. anomolus.AG	*H. fuscopinna.GoO*	*-1.235*	*-1.736*	*-0.754*
C. anomolus.AG	*H. vulgaris.GoO*	*-0.080*	*-0.549*	*0.384*
E. pulcher.AG	*E. ventermaculus.AG*	*-1.011*	*-1.313*	*-0.709*
E. pulcher.AG	*E. pulcher.GoO*	*0.137*	*-0.165*	*0.446*
E. pulcher.AG	*E. ventermaculus.GoO*	*-2.003*	*-2.402*	*-1.641*
E. pulcher.AG	*E. guttata.GoO*	*-1.394*	*-1.704*	*-1.076*
E. pulcher.AG	*H. fuscopinna.GoO*	*-1.847*	*-2.206*	*-1.489*
E. pulcher.AG	*H. vulgaris.GoO*	*-0.694*	*-1.010*	*-0.358*
E. ventermaculus.AG	*E. pulcher.GoO*	*1.149*	*0.847*	*1.459*
E. ventermaculus.AG	*E. ventermaculus.GoO*	*-0.990*	*-1.382*	*-0.610*
E. ventermaculus.AG	*E. guttata.GoO*	*-0.381*	*-0.706*	*-0.065*
E. ventermaculus.AG	*H. fuscopinna.GoO*	*-0.836*	*-1.201*	*-0.475*
E. ventermaculus.AG	*H. vulgaris.GoO*	*0.318*	*-0.016*	*0.648*
E. pulcher.GoO	*E. ventermaculus.GoO*	*-2.138*	*-2.526*	*-1.766*
E. pulcher.GoO	*E. guttata.GoO*	*-1.530*	*-1.843*	*-1.213*
E. pulcher.GoO	*H. fuscopinna.GoO*	*-1.985*	*-2.341*	*-1.615*
E. pulcher.GoO	*H. vulgaris.GoO*	*-0.832*	*-1.174*	*-0.519*
E. ventermaculus.GoO	*E. guttata.GoO*	*0.607*	*0.231*	*1.018*
E. ventermaculus.GoO	*H. fuscopinna.GoO*	*0.152*	*-0.260*	*0.582*
E. ventermaculus.GoO	*H. vulgaris.GoO*	*1.307*	*0.895*	*1.691*
E. guttata.GoO	*H. fuscopinna.GoO*	*-0.453*	*-0.822*	*-0.088*
E. guttata.GoO	*H. vulgaris.GoO*	*0.700*	*0.360*	*1.041*
H. fuscopinna.GoO	*H. vulgaris.GoO*	*1.153*	*0.799*	*1.543*

Table S5 | Sample sizes for CT-trials across species and locations. While sample sizes are low for some species, CT-trials have been shown to yield highly reproducible and taxonomically preserved results[144].

Trials	Location	Species	N
CTmax			
	AG	*Coryogalops anomolus*	3
	AG	*Ecsenius pulcher*	10
	AG	*Enneapterygius ventermaculus*	12
	GoO	*Ecsenius pulcher*	10
	GoO	*Enneapterygius ventermaculus*	3
	GoO	*Eviota guttata*	6
	GoO	*Helcogramma fuscopinna*	6
	GoO	*Hetereleotris vulgaris*	10
CTmin			
	AG	*Coryogalops anomolus*	3
	AG	*Ecsenius pulcher*	11
	AG	*Enneapterygius ventermaculus*	10
	GoO	*Ecsenius pulcher*	10
	GoO	*Enneapterygius ventermaculus*	5
	GoO	*Eviota guttata*	9
	GoO	*Helcogramma fuscopinna*	6
	GoO	*Hetereleotris vulgaris*	8

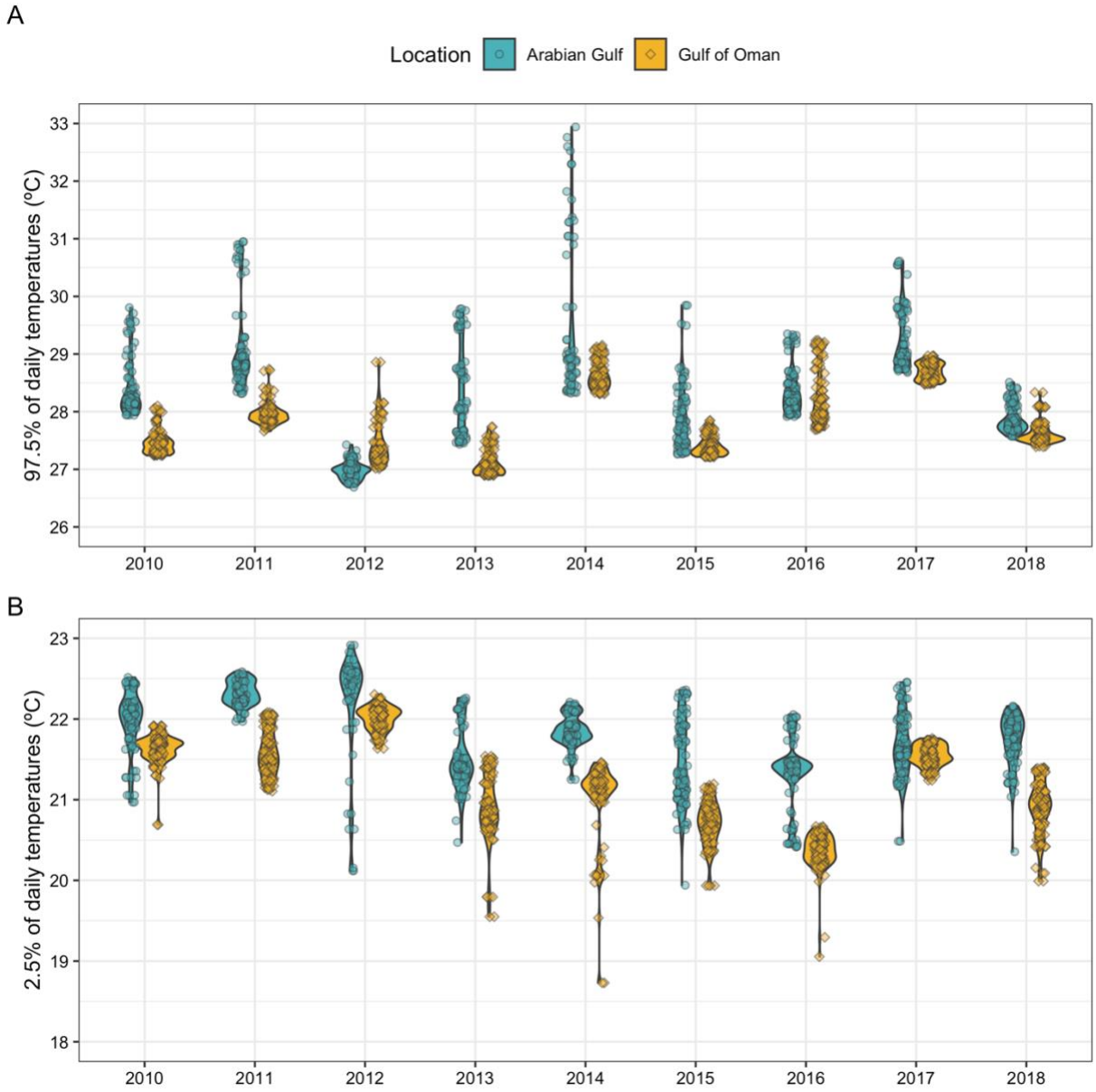

Figure S1 | 97.5% and 2.5% quantiles of remotely sensed temperatures from each year between 2010 and 2018 across our sites in the Arabian Gulf (blue) and Gulf of Oman (gold). Data were sourced from the MODIS-Aqua database (https://oceandata.sci.gsfc.nasa.gov/MODIS-Aqua/Mapped/Daily/4km/sst/2012/).

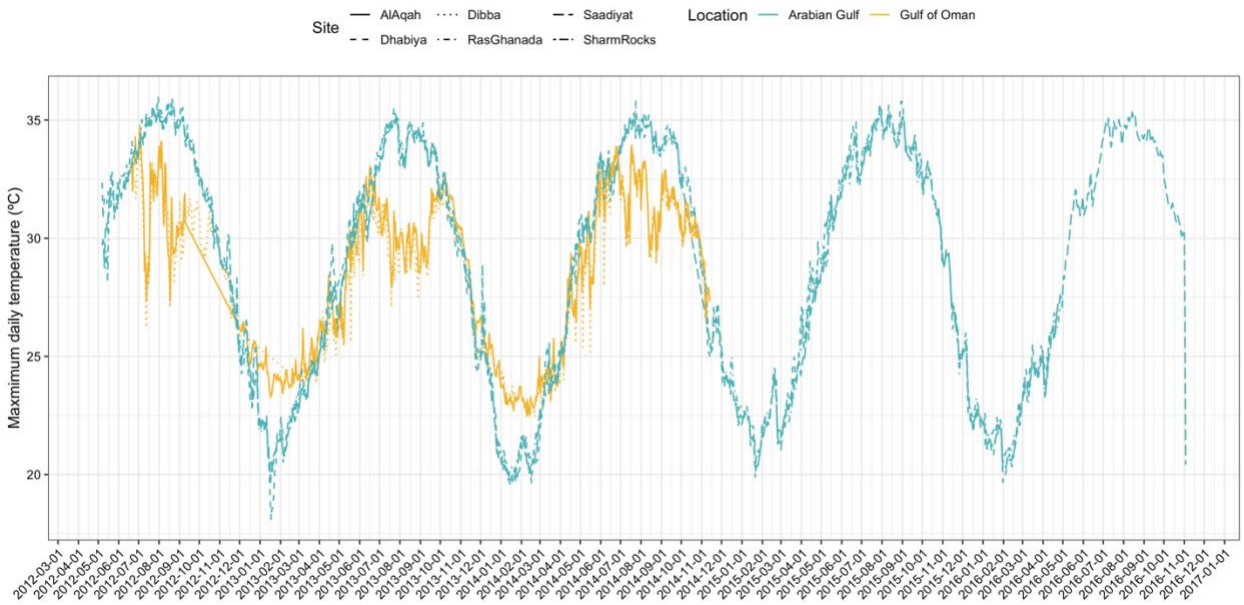

Figure S2 | Temperature records from *in situ* data loggers deployed during various time periods at the six sites across the two locations. Al Aqah = Snoopy Rock.

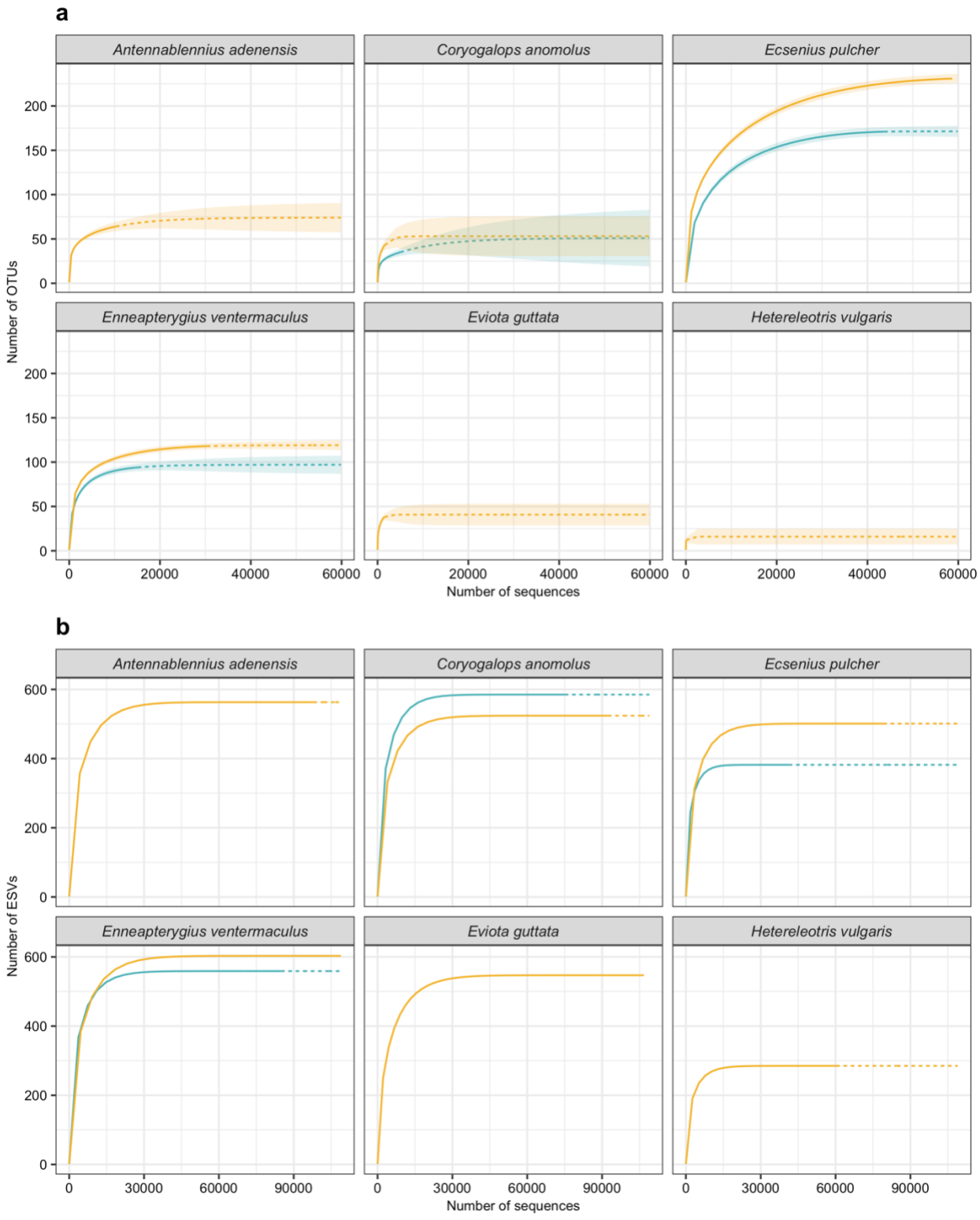

1217

1218 **Figure S3 | Rarefaction curves of OTU and ESV richness across total sequences**
1219 **for six species in the Arabian Gulf (blue) and Gulf of Oman (gold).** (a) OTU
1220 rarefaction curves indicate the diversity of prey items for each species and population

as obtained from gut content DNA metabarcoding with the COI marker, while (b) ESV curves show the diversity of prey items obtained with the 23S marker. Solid lines indicate interpolated richness, while dashed lines indicate extrapolated richness (to the maximum number of sequences across species). Shaded ribbons indicate 95% confidence intervals of extrapolations.